

NWP SAF

Satellite Application Facility for Numerical Weather Prediction

Document NWPSAF-KN-TR-004

Version 1.6



13-08-2021

Two-dimensional variational ambiguity removal (2DVAR)

Jur Vogelzang

KNMI, De Bilt, The Netherlands



 	Two-dimensional variational ambiguity removal (2DVAR)	Doc ID : NWPSAF-KN-TR-004 Version : 1.6 Date : 13-08-2021
--	--	---

Two-dimensional variational ambiguity removal (2DVAR)

Jur Vogelzang

KNMI, The Netherlands

This documentation was developed within the context of the EUMETSAT Satellite Application Facility on Numerical Weather Prediction (NWP SAF), under the Cooperation Agreement dated 29 June 2011, between EUMETSAT and the Met Office, UK, by one or more partners within the NWP SAF. The partners in the NWP SAF are the Met Office, ECMWF, KNMI and Météo France.

Copyright 2012, EUMETSAT, All Rights Reserved.

Change record			
Version	Date	Author / changed by	Remarks
0.1	March 2007	Jur Vogelzang	First draft
0.2	March 2007	Jur Vogelzang	Chapter 5 rewritten
0.3	June 2007	Jur Vogelzang	Added analytical expression for single observation analysis
1.0	August 2007	Jur Vogelzang	First public version
1.1	April 2013	Jur Vogelzang	Corrected some typo's
1.2	September 2013	Jur Vogelzang	Corrected some typo's, improved readability of equations in chapters 2, 3, 4, and 9.
1.3	July 2015/Oct 2016	Jur Vogelzang	Corrected (3.8) and (3.9), added chapter 10, reformulated appendix B.
1.4	May 2017	Jur Vogelzang	Revised and extended appendices for single observation analysis; corrected several errors.
1.5	December 2018	Jur Vogelzang	Corrected typo, extended Appendix F
1.6	August 2021	Jur Vogelzang	Adapted to new 2DVAR grid definition; improved description of how observations enter the 2DVAR analysis; corrected definitions of background error variances.


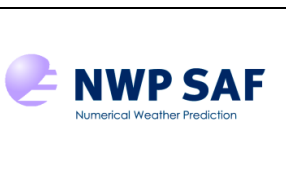
Contents

1	Introduction	5
2	Formulation of the problem	7
3	Transformation of the cost function	11
4	Gradient of the cost function	17
5	Packing in the frequency domain	19
6	Error covariance model	25
7	Single observation test	27
8	Some implementation notes	33
9	Resume	35
10	Flow dependent background errors	39
	Appendix A Fourier transformation	43
	Appendix B Helmholtz transformation	45
	Appendix C Helmholtz transformation in three dimensions	51
	Appendix D Adjoint model	53
	Appendix E Single observation analysis	55
	Appendix F Single observation analysis for EBECs	63
	Appendix G Fourier transforms involving a Gaussian function	67
	Appendix H Minimization step size	71
	References	73



Two-dimensional variational ambiguity removal (2DVAR)

Doc ID : NWPSAF-KN-TR-004
Version : 1.6
Date : 13-08-2021

 	Two-dimensional variational ambiguity removal (2DVAR)	Doc ID : NWPSAF-KN-TR-004 Version : 1.6 Date : 13-08-2021
---	---	---

1 Introduction

Scatterometry

Spaceborne scatterometers are able to measure the surface wind over the oceans at global coverage with a resolution of about 25 km. The surface wind vector is obtained from numerical inversion of the geophysical model function (GMF), an empirical relation between wind vector and observation geometry on one hand and radar backscatter of the ocean surface on the other [Stoffelen, 1998; Portabella, 2002]. If n observations of the radar backscatter are available, each differing from the others in (at least) incidence angle, azimuth angle, radar frequency or polarization, then the GMF defines a folded surface of dimension $n - 12$ in n -dimensional measurement space, where wind speed and wind direction vary along the 2-dimensional surface. The measured wind vector corresponds to the point on the GMF surface that lies closest to the measurement point.

Normally, this procedure does not lead to a unique solution, because the measurements are noisy and because the GMF surface may fold to itself, for example the upwind and downwind surfaces may be in close proximity of each other. For ERS and ASCAT, for instance, the GMF in measurement space takes the form of a folded cone with two sheets; the distance between the sheets being smaller than the typical size of the measurement error.


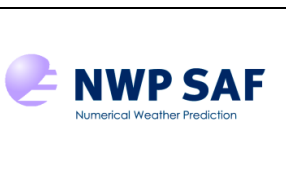
In the multi solution scheme (MSS), the possible solutions are not restricted to those points on the GMF that have minimum distance to the measurement point. In the MSS a large number of a priori probable points on the GMF is retained, up to 144, and the probability of a certain GMF point being the correct solution is proportional to its distance to the measurement point.

The process of selecting the most probable solution is called ambiguity removal. Several schemes have been proposed [Stoffelen, 1998; Portabella, 2002], and a number of schemes is implemented in the genscat library of KNMI, which lies at the base of the scatterometer processors for Ku-band systems like SeaWinds, OSCAT, RapidScat, and HY-2 (PenWP) and for the C-band systems ASCAT (AWDP) that are developed within the NWPSAF project.

Aims and scope

This report describes one of the ambiguity removal methods called two-dimensional variational ambiguity removal (2DVAR). 2DVAR uses a model prediction (either the NCEP model or the ECMWF model) to estimate the best solution. The resulting wind field is constrained by basic physical laws.

The report is detailed and technical. It is intended for understanding the 2DVAR implementation in genscat from the mathematical and methodological point of view. The modules, routines, and data structures are described in the user manuals of PenWP and AWDP [Verhoef *et al.*, 2018a,b].

 	Two-dimensional variational ambiguity removal (2DVAR)	Doc ID : NWPSAF-KN-TR-004 Version : 1.6 Date : 13-08-2021
---	--	---

Overview

Chapter 2 starts with the formulation of the 2DVAR problem. The cost function is introduced as well as the grid on which the 2DVAR problem is solved.

Chapter 3 shows how the background part of the cost function can be transformed such that it becomes a diagonal quadratic form. The resulting transformation, called the conditioning transformation, consists of a Fourier transformation and a Helmholtz transformation of the square root of the background error covariance matrix defined in terms of the velocity potential and the stream function in wavenumber space. It greatly reduces the numerical load. The use of standard FFT algorithms leads to an efficient implementation.

The variational problem is solved by numerically minimizing the cost function expressed in terms of the velocity potential and the stream function in the frequency domain. The minimization procedure is of a quasi Newton type and needs the gradient of the cost function. Chapter 4 shows how the gradient of the cost function is obtained using the so-called adjoint model. In terms of linear algebra, the adjoint of a matrix is its Hermitian conjugate, i.e., the complex conjugate of its transpose. In chapter 4 the adjoint model for 2DVAR is derived.



Chapter 5 deals with the subtleties involved in going from the spatial domain to the frequency domain and vice versa using FFT algorithms. These are caused by the fact that the wind component fields in the spatial domain are real, whereas those in the frequency domain are complex. Symmetry relations keep the number of independent field components the same in both representations, but packing of the independent field components in the frequency domain into a control vector requires careful bookkeeping that also affects the calculation of the cost function and its gradient.

Chapter 6 describes the error covariance model for the background (model) wind field which determines to a large extent the behaviour of 2DVAR. The background error correlations are frequently referred to as structure functions.

Chapter 7 describes how the 2DVAR implementation can be tested with the so-called single observation test. This problem can be solved analytically, and proved to be of crucial importance for getting the normalizations in the genscat 2DVAR implementation right. It is shown how the definition of the structure functions affects the 2DVAR analysis. The convergence properties of the numerical minimization are discussed.

Chapter 8 lists some notes on the 2DVAR implementation in genscat. The report ends with a resume of the most important equations defining 2DVAR. Chapter 9 goes deeper into the choices made in selecting the structure of the background error correlations. The appendices contain a number of detailed derivations that may obscure the main line of reasoning in the text.

Special thanks to Weicheng Ni for finding an error in the equations of chapter 6.

 	Two-dimensional variational ambiguity removal (2DVAR)	Doc ID : NWPSAF-KN-TR-004 Version : 1.6 Date : 13-08-2021
---	---	---

2 Formulation of the problem

General

The probability that \mathbf{x} expresses the true state of the surface wind field given a vector of possible scatterometer wind solutions (ambiguities) \mathbf{v}_o^k equals $P(\mathbf{x} \cap \mathbf{v}_o^k)$. It satisfies [Lorenc, 1986]

$$P(\mathbf{x} \cap \mathbf{v}_o^k) \propto P(\mathbf{v}_o^k | \mathbf{x}) P(\mathbf{x} | \mathbf{x}_b) \quad , \quad (2.1)$$

where $P(\mathbf{v}_o^k | \mathbf{x})$ is the conditional probability that the ambiguous scatterometer wind solutions \mathbf{v}_o^k are observed given the state vector \mathbf{x} , with k the ambiguity index, and $P(\mathbf{x} | \mathbf{x}_b)$ is the conditional probability that \mathbf{x} represents the surface wind field given \mathbf{x}_b , the prior background information (i.e., a model prediction of the wind field). The state vector \mathbf{x} is called the analysis. The most likely estimate of \mathbf{x} is found by maximizing (2.1), or, equivalently, minimizing the cost function J given by

$$J(\mathbf{v}_o^k, \mathbf{x}, \mathbf{x}_b) = -2 \ln P(\mathbf{v}_o^k | \mathbf{x}) - 2 \ln P(\mathbf{x} | \mathbf{x}_b) \quad . \quad (2.2)$$

More detailed information on the scatterometry problem can be found in [Stoffelen, 1998] and [Portabella, 2002]. A description of the 2DVAR method has been given by De Vries *et al.* [2005]

Incremental formulation

To increase the computational efficiency of 2DVAR, the analysis increments $\delta\mathbf{x}$ are used rather than the state vector \mathbf{x} itself, with

$$\delta\mathbf{x} = \mathbf{x} - \mathbf{x}_b \quad , \quad (2.3a)$$

and

$$\delta\mathbf{v}^k = \mathbf{v}_o^k - \mathbf{x}_b \quad . \quad (2.3b)$$

This is called the incremental formulation. For each scatterometer observation the background field is assumed to be known at the same position and time, if necessary from interpolation. The result is that the 2DVAR procedure starts from the model wind field as a first guess. The cost function can be rewritten as

$$J(\delta\mathbf{v}^k, \delta\mathbf{x}) = J_o(\delta\mathbf{v}^k, \delta\mathbf{x}) + J_b(\delta\mathbf{x}) \quad , \quad (2.4)$$

with J_o the observational term and J_b the background term.

Packing

The analysis wind field in 2DVAR is calculated on a regular grid which encompasses all observations. The analysis wind components are packed in the state vector \mathbf{x} (or $\delta\mathbf{x}$ in the incremental approach) which is used in the minimization procedure. In that context, the state vector is also referred to as the control vector. Suppose the 2DVAR analysis grid is defined as

$$(x_{ij}, y_{ij}) \quad , \quad i = 1, 2, \dots, N_1 \quad , \quad j = 1, 2, \dots, N_2 \quad , \quad (2.5)$$

with x_{ij}, y_{ij} the coordinates of the grid point with indices i and j . The analysis or control vectors \mathbf{x} and $\delta\mathbf{x}$ have $2N_1N_2$ components that are ordered as indicated in figure 2.1, with

$$u_{ij} = u(x_{ij}, y_{ij}) \quad , \quad v_{ij} = v(x_{ij}, y_{ij}) \quad , \quad (2.6a)$$

$$\delta u_{ij} = u(x_{ij}, y_{ij}) - u_b(x_{ij}, y_{ij}) \quad , \quad \delta v_{ij} = v(x_{ij}, y_{ij}) - v_b(x_{ij}, y_{ij}) \quad , \quad (2.6b)$$

where (u_{ij}, v_{ij}) is the analysis field and $(\delta u_{ij}, \delta v_{ij})$ the incremental analysis field.

λ	1	2	...	N_1N_2	$N_1N_2 + 1$...	$2N_1N_2$
\mathbf{x}_λ	u_{11}	u_{12}	...	$u_{N_1N_2}$	v_{11}	...	$v_{N_1N_2}$
$\delta\mathbf{x}_\lambda$	δu_{11}	δu_{12}	...	$\delta u_{N_1N_2}$	δv_{11}	...	$\delta v_{N_1N_2}$

Figure 2.1 Packing of the velocity field variables into control vectors.

The order of the elements in the control vector is not relevant for the minimization procedure itself, but it will help to facilitate the derivation in the next sections. Note that the wind fields are packed according to their component and not according to their position.

The background term

Assuming that the errors in the background wind field are Gaussian

$$P(\delta\mathbf{x}) \propto \exp \left[-\frac{1}{2} (\delta\mathbf{x})^T \mathbf{B}^{-1} (\delta\mathbf{x}) \right] \quad , \quad (2.7)$$

with \mathbf{B} the matrix of background wind error covariances and the superscript T indicating that the transpose of the vector or matrix should be taken. This yields

$$J_b(\delta\mathbf{x}) = (\delta\mathbf{x})^T \mathbf{B}^{-1} (\delta\mathbf{x}) + C \quad , \quad (2.8)$$



with C a constant that may be neglected during minimization. Note that taking the transpose suffices since $\delta\mathbf{x}$ is a real vector. In the general case the Hermitian conjugate (complex conjugate of the transpose) should be taken.

In terms of the unpacked velocity fields, the background term of the cost function reads

$$J_b = \sum_{i,j=1}^{N_1,N_2} B_{ij}^{-1} (\delta u_{ij}^2 + \delta v_{ij}^2) \quad . \quad (2.9)$$

This equation holds if the background field is considered as a discrete quantity on a grid. If it is considered as a continuous field, the background cost function reads

$$J_b = \int_{-\infty}^{\infty} \int_{-\infty}^{\infty} dx dy \int_{-\infty}^{\infty} \int_{-\infty}^{\infty} dx' dy' \left[\delta u(x, y) B^{-1}(x, y, x', y') \delta u(x', y') + \delta v(x, y) B^{-1}(x, y, x', y') \delta v(x', y') \right] \quad . \quad (2.10)$$

 	Two-dimensional variational ambiguity removal (2DVAR)	Doc ID : NWPSAF-KN-TR-004 Version : 1.6 Date : 13-08-2021
---	--	---

In 2DVAR the second point of view is taken, assuming that all quantities are sampled on a grid that is large and dense enough to assure convergence of the integrals.

The observational term

The observational term in 2DVAR is most easily expressed in terms of the orthogonal components of the horizontal wind vector fields. It reads [*Stoffelen and Anderson, 1997*]

$$P(\mathbf{v}_0^k | \mathbf{x}) \propto \sum_k p_k \exp \left[-\frac{1}{2} (\delta \mathbf{v}^k)^T (\mathbf{O} + \mathbf{F})^{-1} (\delta \mathbf{v}^k) \right] , \quad (2.11)$$

where the summation extends over all possible solutions (ambiguities). In (2.11), \mathbf{O} stands for the covariance of the observation errors and \mathbf{F} for that of the representation errors (errors caused by spatial and temporal differences between observation and background). The probability of ambiguity number k being the correct solution is given by p_k .

The observation cost function in terms of the unpacked wind velocities reads

$$J_o = \sum_{m=1}^{N_{obs}} \left[\sum_{k=1}^{M_l} \left(\frac{(\delta \bar{u}_m - \delta u_{m,k}^{(o)})^2}{\varepsilon_u^2} + \frac{(\delta \bar{v}_m - \delta v_{m,k}^{(o)})^2}{\varepsilon_v^2} - 2 \ln P_k \right)^{-p} \right]^{-1/p} , \quad (2.12)$$

where the summation is over all N_{obs} observations and all M_l ambiguities of observation m . Equation (2.12) applies in particular to scatterometer observations which in general have M_l ambiguous solutions, each with a-priori probability P_k . Further, ε_u and ε_v are the expected standard deviation of the scatterometer wind components. For all scatterometers $\varepsilon_u = \varepsilon_v = 1.8$ m/s. The parameter p is an empirical parameter that gives optimal separation between multiple solutions for $p = 4$. The analysis increment wind components $\delta \bar{u}_m$ and $\delta \bar{v}_m$ are interpolated to the position of the observation, the interpolation being indicated by the bar. That is why all observations should be contained in the 2DVAR analysis grid with positions (x_{ij}, y_{ij}) as defined in (2.5).


Note that if there is only one single observation present with unit probability, (2.12) reduces to

$$J_o^{SO} = \frac{(\delta u_1 - \delta u_{1,1}^{(o)})^2}{\varepsilon_u^2} + \frac{(\delta v_1 - \delta v_{1,1}^{(o)})^2}{\varepsilon_v^2} . \quad (2.13)$$

The 2DVAR analysis grid

The wind speed vector components are usually given as the west-to-east (zonal) component u and the south-to-north (meridional) component v . 2DVAR uses the transversal wind speed t , perpendicular to the satellite track, and the longitudinal wind speed l , parallel to the satellite track. They are related to u and v by

$$\begin{aligned} t &= u \cos \theta_{ij} + v \sin \theta_{ij} \\ l &= -u \sin \theta_{ij} + v \cos \theta_{ij} \end{aligned} , \quad (2.14)$$

<div data-bbox="140 129 255 185"> The EUMETSAT Network of Satellite Application Facilities </div> <div data-bbox="284 138 550 212">  NWP SAF Numerical Weather Prediction </div>	<h1>Two-dimensional variational ambiguity removal (2DVAR)</h1>	Doc ID : NWPSAF-KN-TR-004 Version : 1.6 Date : 13-08-2021
---	--	---

where θ_{ij} is the orientation of the wind vector cell (WVC) with indices (i, j) , measured counterclockwise from the north. It varies continuously from WVC to WVC, slowly near the equator and more rapidly near the poles. Vogelzang [2006] compares various methods to obtain the orientation of a WVC given its coordinates.

Since the relation between (u, v) and (t, l) is an ordinary rotation, the cost function does not change value or form under this change of variables. Note that t and l have the same role in the 2DVAR batch grid as u and v in a geographical grid. Therefore the transversal and longitudinal wind speed components are often referred to as u and v in the 2DVAR software.

The 2DVAR analysis grid, also referred to as the 2DVAR batch grid since the scatterometer observations are split in so-called batches that span at most one-sixth of an orbit, is more or less aligned with the satellite orbit. It is constructed as follows:

1. The center point of the first row of observations, \mathbf{c}_1 and that of the last row of observations, \mathbf{c}_2 is calculated.
2. A great circle C_{12} is defined through \mathbf{c}_1 and \mathbf{c}_2 . This is the backbone of the grid.
3. The grid points are defined on great circles perpendicular to the backbone C_{12} . The grid is also extended before \mathbf{c}_1 and after \mathbf{c}_2 in order to make the grid large enough.

See Vogelzang [2019] for more details.

3 Transformation of the cost function

Overview

Equations (2.10) and (2.12) completely specify the background and observational part of the cost function, respectively. Both equations are assumed to be formulated in terms of the transversal and longitudinal wind components (t, l) . The total cost function can be calculated once a form for the background wind covariance matrix \mathbf{B} and an efficient way to compute its inverse \mathbf{B}^{-1} are established. This can be achieved by a series of transformations:

- Fourier transformation of the wind field from the spatial domain to the frequency domain;
- Helmholtz transformation from wind fields to potential fields in the frequency domain;
- Normalization with the error covariances (error variances and error autocorrelations).

These three transformations together are called the preconditioning transformation. Its effect is to transform \mathbf{B} expressed in terms of the wind components (t, l) in the spatial domain into the identity matrix in terms of the normalized potential fields $(\hat{\chi}^{(n)}, \hat{\psi}^{(n)})$ in the frequency domain.

The wind error covariances are calculated from the wind vectors at two points. Following *Daley* [1991] it is assumed that the covariances are homogeneous (i.e., independent of the absolute location of the pair of points) and isotropic (i.e., only dependent on the distance between the points). In that case the matrix \mathbf{B} is symmetric and positive definite, so its inverse certainly exists. With $\langle \dots \rangle$ denoting the wind error covariance, the matrix \mathbf{B} can be written in terms of the wind components in the spatial domain as

$$\mathbf{B}_{t,l} = \begin{pmatrix} \langle \delta t, \delta t^T \rangle & \langle \delta t, \delta l^T \rangle \\ \langle \delta l, \delta t^T \rangle & \langle \delta l, \delta l^T \rangle \end{pmatrix} = \begin{pmatrix} B_{tt} & B_{tl} \\ B_{lt} & B_{ll} \end{pmatrix} . \quad (3.1)$$

The background contribution to the cost function reads, see (2.8)


$$J_b = \delta \mathbf{x}^T \mathbf{B}_{t,l}^{-1} \delta \mathbf{x} , \quad (3.2)$$

which can be interpreted as a summation like in (2.9) or an integration like in (2.10)

Fourier transformation

The first step in the preconditioning is to go from the spatial domain to the frequency domain by Fourier transformation (denoted by F). This transforms the matrix-vector multiplications from convolutional form to ordinary multiplication form. The transformation reads $\delta \hat{t} = F \delta t$ and $\delta \hat{l} = F \delta l$, the hat indicating that the quantity is in the frequency domain. On a regular grid with grid size Δx in the position domain and grid size $\Delta p = (N \Delta x)^{-1}$ in the frequency domain, with N the number of grid points, the discrete Fourier transformation and its inverse of a function f in two dimensions read [*Press et al*, 1988]

$$\hat{f}_{k,l} = \Delta^2 \sum_{m=1}^M \sum_{n=1}^N f_{m,n} e^{2\pi i \left(\frac{km}{M} + \frac{ln}{N} \right)} , \quad (3.3a)$$

<div style="display: flex; align-items: center;"> <div style="margin-right: 20px;"> <small>The EUMETSAT Network of Satellite Application Facilities</small> </div> <div>  NWP SAF <small>Numerical Weather Prediction</small> </div> </div>	<h2>Two-dimensional variational ambiguity removal (2DVAR)</h2>	Doc ID : NWPSAF-KN-TR-004 Version : 1.6 Date : 13-08-2021
--	--	---

$$f_{m,n} = \frac{1}{MN\Delta^2} \sum_{k=1}^M \sum_{l=1}^N \hat{f}_{k,l} e^{-2\pi i \left(\frac{km}{M} + \frac{ln}{N} \right)} , \quad (3.3b)$$

where $\Delta = \Delta x = \Delta y$. Note that the normalization factor for the inverse transform equals the grid sizes in frequency space. See appendix A for more detailed information on the Fourier transform.

After Fourier transformation, the background contribution to the cost function reads

$$J_b = \delta \hat{\mathbf{x}}^T \mathbf{B}_{\hat{\mathbf{t}}, \hat{\mathbf{l}}}^{-1} \delta \hat{\mathbf{x}} , \quad (3.4)$$

with $\delta \hat{\mathbf{x}}$ the control vector in the frequency domain.

Helmholtz transformation

The second step is to express the wind speed increments $(\delta \hat{\mathbf{t}}, \delta \hat{\mathbf{l}})$ in the frequency domain in terms of the velocity potential and the stream function $(\delta \hat{\chi}, \delta \hat{\psi})$ by using the inverse transformation.

The forward operator $\mathbf{H} = (H_1, H_2)$ for continuous functions in the spatial domain reads

$$t(x, y) = H_1[\chi, \psi](x, y) = \frac{\partial \chi(x, y)}{\partial x} - \frac{\partial \psi(x, y)}{\partial y} , \quad (3.5a)$$

$$l(x, y) = H_2[\chi, \psi](x, y) = \frac{\partial \chi(x, y)}{\partial y} + \frac{\partial \psi(x, y)}{\partial x} , \quad (3.5b)$$

with the square brackets indicating a function as argument of an operator. Note that the forward transformation transforms potentials into horizontal wind components, while the inverse transformation transforms horizontal wind components into potentials. In appendix B it is shown that the forward transformation in the frequency domain reads

$$\hat{t}(p, q) = \hat{h}(p) \hat{\chi}(p, q) - \hat{h}(q) \hat{\psi}(p, q) , \quad (3.6a)$$

$$\hat{l}(p, q) = \hat{h}(q) \hat{\chi}(p, q) + \hat{h}(p) \hat{\psi}(p, q) , \quad (3.6b)$$

with

$$\hat{h}(p) = -2\pi i p . \quad (3.7)$$

It will be shown later that 2DVAR only needs the forward transformation and its complex conjugate, but expressed on a discrete grid. Equations (3.6) and (3.7) are immediately discretized to


$$\hat{t}_{m,n} = -2\pi i [\hat{p}_m \hat{\chi}_{m,n} - \hat{q}_n \hat{\psi}_{m,n}] , \quad (3.8a)$$

$$\hat{l}_{m,n} = -2\pi i [\hat{q}_n \hat{\chi}_{m,n} + \hat{p}_m \hat{\psi}_{m,n}] , \quad (3.8b)$$

with

$$p_m = \frac{m}{N_1 \Delta} , \quad q_n = \frac{n}{N_2 \Delta} , \quad (3.9)$$

the spatial frequencies resulting from the discrete Fourier transformation.

 	Two-dimensional variational ambiguity removal (2DVAR)	Doc ID : NWPSAF-KN-TR-004 Version : 1.6 Date : 13-08-2021
---	--	---

Definition of the background error covariance matrix

After the inverse Helmholtz transformation, the background contribution to the cost function is given by

$$J_b = \delta \xi^T B_{\hat{\psi}, \hat{\chi}}^{-1} \delta \xi \quad , \quad (3.10)$$

with $\delta \xi$ the control vector in terms of the velocity potential and the stream function in the frequency domain.

The error covariance matrix given by

$$B_{\hat{\chi}, \hat{\psi}} = \begin{pmatrix} \langle \delta \hat{\chi}, \delta \hat{\chi}^T \rangle & \langle \delta \hat{\chi}, \delta \hat{\psi}^T \rangle \\ \langle \delta \hat{\psi}, \delta \hat{\chi}^T \rangle & \langle \delta \hat{\psi}, \delta \hat{\psi}^T \rangle \end{pmatrix} = \begin{pmatrix} B_{\hat{\chi}\hat{\chi}} & B_{\hat{\chi}\hat{\psi}} \\ B_{\hat{\psi}\hat{\chi}} & B_{\hat{\psi}\hat{\psi}} \end{pmatrix} \quad . \quad (3.11)$$

The advantage of applying these transformations is that the cross covariances in B , the ones between δu and δv , that are not negligible in terms of the horizontal wind components in the spatial domain become almost zero,

$$B_{\hat{\chi}, \hat{\psi}} \approx \begin{pmatrix} B_{\hat{\chi}\hat{\chi}} & 0 \\ 0 & B_{\hat{\psi}\hat{\psi}} \end{pmatrix} \quad . \quad (3.12)$$

Now, the matrix has become diagonal. The last step is to factorize it into error variances Σ and error correlations Γ by

$$B_{\hat{\chi}, \hat{\psi}} = \Sigma \Gamma \Sigma \quad , \quad (3.13)$$

with

$$\Sigma = \begin{pmatrix} \Sigma_{\hat{\chi}} & 0 \\ 0 & \Sigma_{\hat{\psi}} \end{pmatrix} \quad , \quad \Gamma = \begin{pmatrix} \Gamma_{\hat{\chi}\hat{\chi}} & 0 \\ 0 & \Gamma_{\hat{\psi}\hat{\psi}} \end{pmatrix} \quad . \quad (3.14)$$

The stream function and the velocity potential are not observable quantities, but their error variances and error correlations can be derived from the wind field, either from theory or from measurements (or a combination of the two). See section 6 for more information.

Once the matrix is diagonal, it is inverted easily: the inverse matrix is also diagonal and each diagonal element in the inverse matrix is the inverse of the corresponding element in the original matrix. Also the square root of a diagonal matrix can be easily found: it is a diagonal matrix in which each diagonal element equals the square root of the original element. The background contribution to the cost function finally reads

$$J_b = \delta \hat{\xi}^T B_{\hat{\chi}, \hat{\psi}}^{-1} \delta \hat{\xi} = \delta \hat{\xi}^T B_{\hat{\chi}, \hat{\psi}}^{-1/2} B_{\hat{\chi}, \hat{\psi}}^{-1/2} \delta \hat{\xi} \quad . \quad (3.15)$$

In the original formulation in the spatial domain, equation (2.8) evaluation of the cost function would require a full matrix-vector multiplication, whereas in the frequency domain only multiplication with the diagonal components is required (convolutional form). Therefore this step is also referred to as convolution.

Preconditioning and unconditioning transformation

The transformations can be combined to the so-called preconditioning transformation

$$\xi = B_{\hat{\chi}, \hat{\psi}}^{-1/2} H^{-1} F \delta x = C \delta x \quad , \quad (3.16)$$

where ξ is the preconditioned state vector. It is obtained from packing the increments in the potential fields in the frequency domain, normalized with the square root of the error variances and error correlations. This is the state vector actually used in the 2DVAR minimization process, and therefore the inverse of (3.16) is needed in 2DVAR. This is called the unconditioning transformation \mathbf{U} and it satisfies

$$\delta \mathbf{x} = \mathbf{F}^{-1} \mathbf{H} \mathbf{B}_{\hat{\chi}, \hat{\psi}}^{1/2} \xi = \mathbf{U} \xi \quad . \quad (3.17)$$

Figure 3.1 shows the unconditioning transformation schematically.

$$J_b = \Delta p \Delta q \sum_{\lambda} w_{\lambda} \xi_{\lambda}^2 \quad , \lambda w_{\lambda}$$

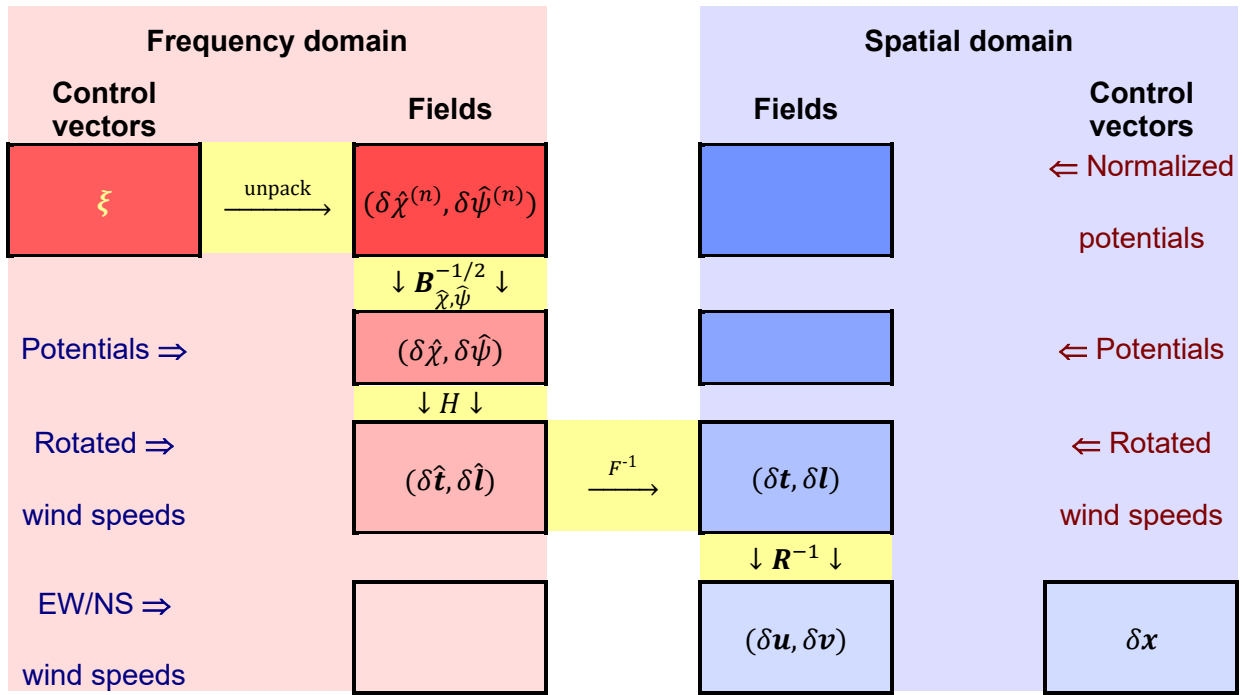



Figure 3.1 Scheme of the unconditioning transformation (the yellow path).

The preconditioning transformation reduces the background error covariance matrix to the identity matrix, so the background cost function is expected to become simply the scalar product of the conditioned control vector with itself. In chapter 5 it will be shown that there are some subtleties involved due to the nature of the numerically calculated Fourier transform. The final form of the background cost function equals

$$J_b = \Delta p \Delta q \sum_{\lambda} w_{\lambda} \xi_{\lambda}^2 \quad , \quad (3.18)$$

with the index λ running over all components of the control vector and the weights w_{λ} determined by the symmetry properties of the Fourier transform (see chapter 5).

<div style="display: flex; align-items: center;"> <div style="margin-right: 20px;"> <small>The EUMETSAT Network of Satellite Application Facilities</small> </div> <div>  NWP SAF <small>Numerical Weather Prediction</small> </div> </div>	<h2 style="margin: 0;">Two-dimensional variational ambiguity removal (2DVAR)</h2>	Doc ID : NWPSAF-KN-TR-004 Version : 1.6 Date : 13-08-2021
--	---	---

The origin of the normalization factor in front of the summation in (3.18) can be understood by writing the background cost function in terms of the normalized potential fields in the frequency domain, $\hat{\psi}^{(n)}$ and $\hat{\chi}^{(n)}$, as

$$J_b = \int_{-\infty}^{\infty} \int_{-\infty}^{\infty} dp dq [\hat{\psi}^{(n)}(p, q)]^2 + [\hat{\chi}^{(n)}(p, q)]^2 \quad . \quad (3.19)$$

If (3.19) is evaluated on a regular grid using first-order quadrature (higher order is not necessary since the FFT algorithm used for the Fourier transformation is also first-order) one obtains

$$J_b = \sum_{i=1}^N \Delta p \sum_{j=1}^M \Delta q [\hat{\psi}^{(n)}(p_i, q_j)]^2 + [\hat{\chi}^{(n)}(p_i, q_j)]^2 \quad , \quad (3.20)$$


where the factor $\Delta p \Delta q$ can be moved in front of the summation. See also chapter 5.



The observation term remains the same,

$$J_o = \sum_{m=1}^{N_{obs}} \left[\sum_{k=1}^{M_l} \left(\frac{(\delta \bar{t}_m - \delta t_{m,k}^{(o)})^2}{\varepsilon_t^2} + \frac{(\delta \bar{l}_m - \delta l_{m,k}^{(o)})^2}{\varepsilon_l^2} - 2 \ln P_k \right)^{-p} \right]^{-1/p} \quad , \quad (3.21)$$

with $\varepsilon_t = \varepsilon_l = 1.8$ m/s and the bar indicating interpolation of the analysis wind components to the position of the observation.

The horizontal wind component increments in the spatial domain, $\delta \bar{t}_m$ and $\delta \bar{l}_m$ are obtained from unpacking, unconditioning, and interpolating the control vector ξ . In this way, all transformations are contained in the background part of the cost function.

<p>The EUMETSAT Network of Satellite Application Facilities</p> 	<h1>Two-dimensional variational ambiguity removal (2DVAR)</h1>	<p>Doc ID : NWPSAF-KN-TR-004 Version : 1.6 Date : 13-08-2021</p>
---	--	--

 	Two-dimensional variational ambiguity removal (2DVAR)	Doc ID : NWPSAF-KN-TR-004 Version : 1.6 Date : 13-08-2021
---	---	---

4 Gradient of the cost function

The minimization is done using routine LBFGS from J. Nocedal [*Liu and Nocedal*, 1989]. This is a freeware routine for minimization using the limited memory BFGS method. The routine not only needs the value of the cost function for arbitrary values of the control vector, but also its gradient with respect to the control vector.

The background term

The background contribution to the cost function is given by (3.18) and reads

$$J_b = \Delta_p \Delta_q \sum_{\lambda} w_{\lambda} \xi_{\lambda}^2 \quad . \quad (4.1)$$

This can be considered as a summation or an integral, see (3.19). Its gradient with respect to the control vector is simply

$$\nabla J_b|_{\lambda} = \frac{\partial J_b}{\partial \xi_{\lambda}} = 2\Delta_p \Delta_q w_{\lambda} \xi_{\lambda} \quad , \quad (4.2)$$

which is a vector in preconditioned control vector space. Section 5 addresses the question how to express (4.1) and (4.2) in terms of the normalized potential fields in the frequency domain.

The observation term

The observation contribution to the gradient is

$$\nabla J_o = \frac{\partial J_o}{\partial \xi} \quad , \quad (4.3)$$

which is again a vector in preconditioned control vector space, i.e., the control vector in terms of the normalized potential fields in the frequency domain. This must be transformed to an expression in terms of the velocity fields in the spatial domain (ordinary control vector space), because the observation source term is defined in that representation. In matrix-vector notation this can be written as (see appendix D)

$$\nabla J_o = \mathbf{U}^* \frac{\partial J_o}{\partial \delta x} \quad , \quad (4.4)$$

where \mathbf{U}^* is the adjoint of the preconditioning transformation \mathbf{U} defined in (3.17), i.e., the complex conjugate of the transpose of \mathbf{U} . In appendix D it is also shown that


$$\mathbf{U}^* = \overline{\mathbf{U}^T} = \overline{\left(\mathbf{F}^{-1} \mathbf{H} \mathbf{B}_{\hat{\chi}, \hat{\psi}}^{1/2} \right)^T} = \mathbf{B}_{\hat{\chi}, \hat{\psi}}^{1/2} \mathbf{H}^* \mathbf{F} \quad , \quad (4.5)$$

since the Fourier transform is self-adjoint and the background error correlations are real.

The derivatives of J_o in the spatial domain are easily obtained from (3.20). Writing

$$J_o = \sum_{m=1}^{N_{obs}} J_s^{-1/p} \quad , \quad J_s = \sum_{m=1}^{M_{ij}} \left(\frac{(\delta \bar{t}_m - \delta t_{m,k}^{(o)})^2}{\varepsilon_t^2} + \frac{(\delta \bar{t}_m - \delta t_{m,k}^{(o)})^2}{\varepsilon_l^2} - 2 \ln P_k \right)^{-p} \quad , \quad (4.6)$$

the components of the gradient in the spatial domain equal

<div style="display: flex; align-items: center;"> <div style="margin-right: 20px;"> <small>The EUMETSAT Network of Satellite Application Facilities</small> </div> <div>  NWP SAF <small>Numerical Weather Prediction</small> </div> </div>	<h2 style="margin: 0;">Two-dimensional variational ambiguity removal (2DVAR)</h2>	<div style="font-family: monospace; font-size: 0.9em;"> Doc ID : NWPSAF-KN-TR-004 Version : 1.6 Date : 13-08-2021 </div>
--	---	--

$$\frac{\partial J_o}{\partial \delta \bar{t}_m} = \frac{\partial J_o}{\partial J_s} \frac{\partial J_s}{\partial \delta \bar{t}_m} = \frac{-1}{p} J_s^{-1-1/p} \frac{\partial J_s}{\partial \delta \bar{t}_m} \quad , \quad \frac{\partial J_o}{\partial \delta \bar{l}_m} = \frac{\partial J_o}{\partial J_s} \frac{\partial J_s}{\partial \delta \bar{l}_m} = \frac{-1}{p} J_s^{-1-1/p} \frac{\partial J_s}{\partial \delta \bar{l}_m} \quad , \quad (4.7)$$

with


$$\begin{aligned} \frac{\partial J_s}{\partial \delta \bar{t}_m} &= -p \sum_{k=1}^{M_m} \left(\frac{(\delta \bar{t}_m - \delta t_{m,k}^{(o)})^2}{\varepsilon_t^2} + \frac{(\delta \bar{l}_m - \delta l_{m,k}^{(o)})^2}{\varepsilon_l^2} - 2 \ln P_k \right)^{-p-1} \frac{2(\delta \bar{t}_m - \delta t_{m,k}^{(o)})}{\varepsilon_t^2} \quad , \\ \frac{\partial J_s}{\partial \delta \bar{l}_m} &= -p \sum_{k=1}^{M_m} \left(\frac{(\delta \bar{t}_m - \delta t_{m,k}^{(o)})^2}{\varepsilon_t^2} + \frac{(\delta \bar{l}_m - \delta l_{m,k}^{(o)})^2}{\varepsilon_l^2} - 2 \ln P_k \right)^{-p-1} \frac{2(\delta \bar{l}_m - \delta l_{m,k}^{(o)})}{\varepsilon_l^2} \quad . \end{aligned} \quad (4.8)$$

Note that the factors $-p^{-1}$ and $-p$ in (4.7) and (4.8) cancel. The gradient with respect to the control variables of the observation term is thus obtained by adjoint preconditioning of the gradient in the analysis field in the spatial domain.

In case of one single observation with unit probability, equations (4.6) and (4.7) simplify to

$$J_o^{SO} = \frac{(\delta \bar{t}_1 - \delta t_{1,1}^{(o)})^2}{\varepsilon_t^2} + \frac{(\delta \bar{l}_1 - \delta l_{1,1}^{(o)})^2}{\varepsilon_l^2} \quad , \quad (4.9)$$

$$\frac{\partial J_o^{SO}}{\partial \delta \bar{t}_1} = \frac{2(\delta \bar{t}_1 - \delta t_{1,1}^{(o)})}{\varepsilon_t^2} \quad , \quad \frac{\partial J_o^{SO}}{\partial \delta \bar{l}_1} = \frac{2(\delta \bar{l}_1 - \delta l_{1,1}^{(o)})}{\varepsilon_l^2} \quad . \quad (4.10)$$

<div style="display: flex; align-items: center;"> <div style="margin-right: 20px;"> <small>The EUMETSAT Network of Satellite Application Facilities</small> </div> <div>  NWP SAF <small>Numerical Weather Prediction</small> </div> </div>	<h2 style="margin: 0;">Two-dimensional variational ambiguity removal (2DVAR)</h2>	Doc ID : NWPSAF-KN-TR-004 Version : 1.6 Date : 13-08-2021
--	---	---

5 Packing in the frequency domain

In section 1 it was shown that the control vector in the spatial domain can be defined in terms of the horizontal wind speed components (u_{ij}, v_{ij}) or, equivalently, (t_{ij}, l_{ij}) as depicted in figure 2.1. In particular, the control vector in the spatial domain has dimension $2N_1N_2$. Some care must be taken when defining the control vector in the frequency domain, because of the peculiarities of the Fast Fourier Transform (FFT) algorithm. Before moving to the full problem, some main characteristics will be discussed in a one dimensional example.

One dimensional example

Suppose a real function $f(x)$ with Fourier transform $\hat{f}(p)$. When applying an FFT algorithm, the function f is sampled at N real values in the spatial domain, while \hat{f} is sampled at N complex values in the frequency domain. As discussed by *Press et al.* [1988], these complex numbers are not independent because \hat{f} satisfies the symmetry relation

$$\hat{f}(-p) = \hat{f}^*(p) \quad , \quad (5.1)$$

the star indicating complex conjugation. This can easily be shown from the definition of the Fourier transform (A.1).

On an FFT grid the sampling points in the spatial domain have coordinates x_i given by

$$x_i = (i - 1)\Delta \quad , \quad i = 1, \dots, N \quad , \quad (5.2)$$

assuming a square grid with size Δ . The forward FFT operation returns the coefficients on a frequency grid p_j given by

$$p_j = j\hat{\Delta} \quad , \quad j = -\frac{1}{2}M + 1, \dots, +\frac{1}{2}M \quad , \quad (5.3)$$

where

$$\hat{\Delta} = \frac{1}{N\Delta} \quad . \quad (5.4)$$

Using (5.1), only the non-negative frequencies of p are independent. The FFT algorithm returns the Fourier coefficients in a rather peculiar order [*Press et al.* 1988]. This is shown schematically in figure 5.1. The first coefficient, \hat{f}_1 , corresponds to zero frequency and is therefore real because it is simply the integral over the function f . The next coefficients, \hat{f}_j for $j = 2, \dots, \frac{1}{2}N$, are complex and correspond to frequencies $(j - 1)\hat{\Delta}$. The coefficient with index $j = \frac{1}{2}N + 1$ is the sum of the contributions at plus and minus the maximum frequency $p_{\frac{1}{2}max}$. Because of (5.1) this coefficient is also real. The last coefficients with indices $j = \frac{1}{2}N + 2, \dots, N$ correspond to the negative frequencies $(j - N - 1)\hat{\Delta}$ and these are the complex conjugates of the corresponding coefficients at positive frequency. Note that the coefficients which are each others complex conjugate lie symmetrically around the point with maximum frequency.

\hat{f}_1	\hat{f}_2	\hat{f}_3	\hat{f}_4	\hat{f}_5	$\hat{f}_6 = \hat{f}_4^*$	$\hat{f}_7 = \hat{f}_3^*$	$\hat{f}_8 = \hat{f}_2^*$
$p = 0$	$p = \hat{\Delta}$	$p = 2\hat{\Delta}$	$p = 3\hat{\Delta}$	$p = \pm 4\hat{\Delta}$	$p = -3\hat{\Delta}$	$p = -2\hat{\Delta}$	$p = -\hat{\Delta}$

Figure 5.1 Structure of the one dimensional Fourier coefficients in the frequency domain for $N=8$. The blue cells contain real coefficients, the red cells complex with conjugate pairs in the same shade of red. The frequency is given below.

This implies that the N complex Fourier coefficients in the frequency domain contain exactly N independent real numbers, see also figure 5.1.

Two dimensional case

In the two dimensional case, applicable to 2DVAR, the Fourier transform in the frequency domain, $\hat{f}(p, q)$, of a real function in the spatial domain, $f(x, y)$ satisfies

$$\hat{f}(-p, -q) = \hat{f}^*(p, q) \quad . \quad (5.5)$$

In the spatial domain the 2DVAR batch grid is sampled on points (x_i, y_j) with

$$x_i = (i - 1)\Delta \quad , \quad i = 1, 2, \dots, N_1 \quad , \quad (5.6a)$$

$$y_j = (j - 1)\Delta \quad , \quad j = 1, 2, \dots, N_2 \quad , \quad (5.6b)$$

assuming a square grid. An FFT operation returns the coefficients $\hat{f}_{ij} = \hat{f}(p_i, q_j)$ with

$$p_i = i\hat{\Delta}_p \quad , \quad i = -\frac{1}{2}N_1 + 1, \dots, \frac{1}{2}N_1 \quad , \quad (5.7a)$$

$$q_j = j\hat{\Delta}_q \quad , \quad j = -\frac{1}{2}N_2 + 1, \dots, \frac{1}{2}N_2 \quad , \quad (5.7b)$$

with

$$\Delta_p = \frac{1}{N_1\Delta} \quad , \quad \Delta_q = \frac{1}{N_2\Delta} \quad . \quad (5.8)$$

The ordering of the FFT coefficients in the frequency domain is analogous to the one dimensional case and sketched in figure 5.2.

The coefficients of the first row have $p = 0$ and therefore

$$\hat{f}_{1,j} = \hat{f}(0, q_j) = \int dx dy f(x, y) e^{2\pi i q_j y} = \int dy F_x(y) e^{2\pi i q_j y} \quad , \quad (5.9)$$

with

$$F_x(y) = \int dx f(x, y) \quad . \quad (5.10)$$

Now F_x is a real function, because f is real. Equation (5.9) defines the coefficients of the first row as the FFT coefficients of a real function. The coefficients in the first row therefore satisfy the symmetry relations of the one dimensional case. The coefficients with indices $(1,1)$ and $(1, \frac{1}{2}N_2 + 1)$ are real, while the others are complex and each others complex conjugate, symmetric around the coefficient with index $(1, \frac{1}{2}N_2 + 1)$ as

indicated by the white star in figure 5.2. The same argument holds with x and y interchanged, and therefore the coefficients of the first column are those of a real function.

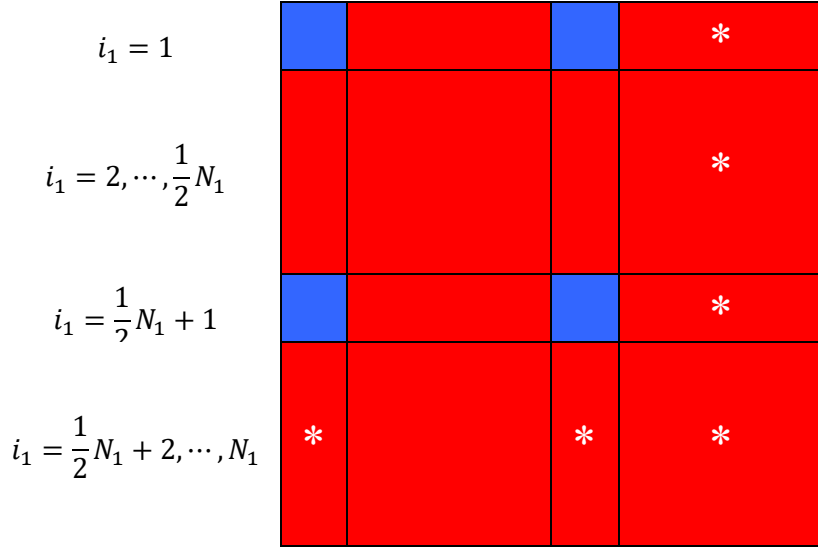


Figure 5.2 Structure of the two dimensional Fourier coefficients of a real function. Real coefficients are indicated in blue, complex coefficients in red. The row numbers are given at the left. The column numbering is analogous. The stars indicate coefficients that are not independent.

The coefficients of row $k_1 = \frac{1}{2}N_1 + 1$ satisfy

$$\hat{f}_{k_1, j} = \hat{f}(p_{\max}, q_j) + \hat{f}(-p_{\max}, q_j) = \iint dx dy f(x, y) \left[e^{2\pi i(p_{\max}x + q_j y)} + e^{2\pi i(-p_{\max}x + q_j y)} \right] , \quad (5.11)$$

with $p_{\frac{1}{2}N_1 + 1}$. This can be written as

$$\hat{f}_{k_1, j} = \int dy e^{2\pi i q_j y} \int dx 2 \cos(p_{\max} x) \quad (5.12)$$

which again is the Fourier transform of a real function. The FFT coefficients in row $\frac{1}{2}N_1 + 1$ therefore satisfy the same symmetry relations as those in row 1. The same argument holds with x and y interchanged, so the FFT coefficients in column $\frac{1}{2}N_2 + 1$ satisfy the same symmetry relations as those in row 1.

The other coefficients are all complex and form complex conjugate pairs. The pairs lie point symmetric around the point with indices $(k_1, k_2) = (\frac{1}{2}N_1 + 1, \frac{1}{2}N_2 + 1)$ due to (5.5). All coefficients in an area marked with a white star in figure 5.2 are the complex conjugate of another one in a non-marked area. In total there are exactly $N_1 N_2$ independent numbers, as can easily be inferred from figure 5.2.

A final point concerns the coefficient with indices (1,1). This coefficient corresponds to zero frequency, and is just the average of the function in the frequency domain. For the normalized potential increment fields in the frequency domain in 2DVAR it represents energy fed into or drained from the wind field. Since 2DVAR

is not allowed to change the energy from the system, this coefficient should be zero. Note that such a change in energy transforms to an average wind in the spatial domain. Putting the coefficient with indices (1,1) in the frequency domain equal to zero is equivalent to the requirement that 2DVAR should be free of bias – a common and reasonable demand.

With this information, the packing and unpacking algorithms can be constructed as indicated in figures 5.3 and 5.4, respectively. The dimension of the control vector equals $2(N_1 N_2 - 1)$. Note that the role of real and imaginary components is opposite of that in the “normal” situation, because the transformation coefficients are purely imaginary.

Basically, the algorithm contains loops over index i_1 running from 1 to the total number of grid points in the first dimension, N_1 , and index i_2 running from 1 to half the number of grid points plus one in the second dimension, $k_2 = \frac{1}{2}N_2 + 1$. The loops are done twice, once for the velocity potential and once for the stream function.

$$\lambda = 0$$

$$k_1 = \frac{1}{2}N_1 + 1 \quad k_2 = \frac{1}{2}N_2 + 1$$

$$i_1 = 1$$

$i_2 = 1$
 $i_2 = 2, \frac{1}{2}N_2$
 $i_2 = k_2$

No action

 $\xi_{\lambda+1} = \text{Im}\hat{\psi}^{(n)}(1, i_2) ; \quad \xi_{\lambda+2} = \text{Re}\psi^{(n)}(1, i_2) \quad \lambda = \lambda + 2$
 $\xi_{\lambda+1} = \text{Im}\hat{\psi}^{(n)}(1, k_2) ; \quad \lambda = \lambda + 1$

$$i_1 = 2, \frac{1}{2}N_1$$

$j_1 = N_1 + 2 - i_1$
 $i_2 = 1$
 $i_2 = 2, \frac{1}{2}N_2$
 $i_2 = k_2$

$\xi_{\lambda+1} = \text{Im}\hat{\psi}^{(n)}(i_1, 1) ; \quad \xi_{\lambda+2} = \text{Re}\psi^{(n)}(i_1, 1) \quad \lambda = \lambda + 2$
 $\xi_{\lambda+1} = \text{Im}\hat{\psi}^{(n)}(i_1, i_2) ; \quad \xi_{\lambda+2} = \text{Re}\psi^{(n)}(i_1, i_2) \quad \lambda = \lambda + 2$
 $\xi_{\lambda+1} = \text{Im}\hat{\psi}^{(n)}(j_1, i_2) ; \quad \xi_{\lambda+2} = \text{Re}\psi^{(n)}(j_1, i_2) \quad \lambda = \lambda + 2$
 $\xi_{\lambda+1} = \text{Im}\hat{\psi}^{(n)}(i_1, k_2) ; \quad \xi_{\lambda+1} = \text{Re}\hat{\psi}^{(n)}(i_1, k_2) \quad \lambda = \lambda + 2$

$$i_1 = k_1$$

$i_2 = 1$
 $i_2 = 2, \frac{1}{2}N_2$
 $i_2 = k_2$

$\xi_{\lambda+1} = \text{Im}\hat{\psi}^{(n)}(k_1, 1) ; \quad \lambda = \lambda + 1$
 $\xi_{\lambda+1} = \text{Im}\hat{\psi}^{(n)}(k_1, i_2) ; \quad \xi_{\lambda+2} = \text{Re}\psi^{(n)}(k_1, i_2) \quad \lambda = \lambda + 2$
 $\xi_{\lambda+1} = \text{Im}\hat{\psi}^{(n)}(k_1, k_2) ; \quad \lambda = \lambda + 1$

Repeat with $\hat{\psi}^{(n)}$ replaced by $\hat{\chi}^{(n)}$

Figure 5.3 Packing algorithm in the frequency domain.

$$\begin{aligned}
&\lambda = 0 \\
&k_1 = \frac{1}{2} N_1 + 1 \quad k_2 = \frac{1}{2} N_2 + 1 \\
&j_1 = N_1 + 2 - i_1 \quad j_2 = N_2 + 2 - i_2 \\
\\
&i_1 = 1 \\
&\quad i_2 = 1 \quad \psi^{(n)}(1,1) = (0,0) \\
&\quad i_2 = 2, \frac{1}{2} N_2 \quad \lambda = \lambda + 2 \quad \psi^{(n)}(1, i_2) = (\xi_\lambda, \xi_{\lambda-1}); \quad \hat{\psi}^{(n)}(1, j_2) = \hat{\psi}^{(n)*}(1, i_2) \\
&\quad i_2 = k_2 \quad \lambda = \lambda + 1 \quad \hat{\psi}^{(n)}(1, k_2) = (0, \xi_\lambda) \\
\\
&i_1 = 2, \frac{1}{2} N_1 \\
&\quad i_2 = 1 \quad \lambda = \lambda + 2 \quad \psi^{(n)}(i_1, 1) = (\xi_\lambda, \xi_{\lambda-1}); \quad \hat{\psi}^{(n)}(j_1, 1) = \hat{\psi}^{(n)*}(i_1, 1) \\
&\quad i_2 = 2, \frac{1}{2} N_2 \quad \lambda = \lambda + 2 \quad \psi^{(n)}(i_1, i_2) = (\xi_\lambda, \xi_{\lambda-1}); \quad \hat{\psi}^{(n)}(j_1, j_2) = \hat{\psi}^{(n)*}(i_1, i_2) \\
&\quad \quad \quad \lambda = \lambda + 2 \quad \psi^{(n)}(j_1, i_2) = (\xi_\lambda, \xi_{\lambda-1}); \quad \hat{\psi}^{(n)}(i_1, j_2) = \hat{\psi}^{(n)*}(j_1, i_2) \\
&\quad i_2 = k_2 \quad \lambda = \lambda + 2 \quad \psi^{(n)}(i_1, k_2) = (\xi_\lambda, \xi_{\lambda-1}); \quad \hat{\psi}^{(n)}(j_1, k_2) = \hat{\psi}^{(n)*}(i_1, k_2) \\
\\
&i_1 = k_1 \\
&\quad i_2 = 1 \quad \lambda = \lambda + 1 \quad \hat{\psi}^{(n)}(k_1, 1) = (0, \xi_\lambda) \\
&\quad i_2 = 2, \frac{1}{2} N_2 \quad \lambda = \lambda + 2 \quad \hat{\psi}^{(n)} = (\xi_\lambda, \xi_{\lambda-1}); \quad \hat{\psi}^{(n)}(1, j_2) = \hat{\psi}^{(n)*}(1, i_2) \\
&\quad i_2 = k_2 \quad \lambda = \lambda + 1 \quad \hat{\psi}^{(n)}(k_1, k_2) = (0, \xi_\lambda) \\
\\
&\text{Repeat with } \hat{\psi}^{(n)} \text{ replaced by } \hat{\chi}^{(n)}.
\end{aligned}$$

Figure 5.4 Unpacking algorithm in the frequency domain.

Effect on the background cost function

The basic form of the background cost function is given by (3.19) as

$$J_b = \int_{-\infty}^{\infty} \int_{-\infty}^{\infty} dp dq [\hat{\psi}^{(n)}(p, q)]^2 + [\hat{\chi}^{(n)}(p, q)]^2 \quad (5.13)$$

Approximating the integral by a first-order summation (just like the integrals for the Fourier transformations in the FFT algorithm), this yields


$$J_b = \Delta_p \Delta_q \sum_{i_1=1}^{N_1} \sum_{i_2=1}^{N_2} [\hat{\psi}^{(n)}(i_1, i_2)]^2 + [\hat{\chi}^{(n)}(i_1, i_2)]^2 \quad (5.14)$$

with the summations running over the 2DVAR batch grid in the frequency domain.

Now we can apply the symmetry relations of the previous sections to the Fourier coefficients $\hat{\psi}^{(n)}$ and $\hat{\chi}^{(n)}$.

The contribution of a conjugate pair equals

$$[\hat{\psi}^{(n)}(i_1, i_2)]^2 + [\hat{\psi}^{(n)}(j_1, j_2)]^2 = 2[\widehat{Re \psi}^{(n)}(i_1, i_2)]^2 + 2 Im[\hat{\psi}^{(n)}(i_1, i_2)]^2 =$$

<div data-bbox="140 129 255 190" data-label="Page-Header"> <p>The EUMETSAT Network of Satellite Application Facilities</p> </div> <div data-bbox="284 143 550 219" data-label="Page-Header">  <p>NWP SAF Numerical Weather Prediction</p> </div>	<p>Two-dimensional variational ambiguity removal (2DVAR)</p>	<p>Doc ID : NWPSAF-KN-TR-004 Version : 1.6 Date : 13-08-2021</p>
--	--	--

$$= 2[\hat{\psi}^{(n)}(i_1, i_2)]^2, \quad (5.15)$$

with $j_1 = N_1 + 2 - i_1$ and $j_2 = N_2 + 2 - i_2$. This explains the origin of the factor w_λ in (3.18). If all independent components of $\hat{\psi}^{(n)}$ and $\hat{\chi}^{(n)}$ are written as components of the control vector ξ according to the packing algorithm in figure 5.3, the background cost function reads

$$J_b = \Delta_p \Delta_q \sum_\lambda w_\lambda \xi_\lambda^2. \quad (5.16)$$

The weights w_λ are equal to 2 if the corresponding element of $\hat{\psi}^{(n)}$ or $\hat{\chi}^{(n)}$ belongs to a conjugate pair, and it equals 1 if that is not the case. This happens only for indices $(1, k_2)$, $(k_1, 1)$, and (k_1, k_2) as can be inferred from figure 5.4. The components with index $(1, 1)$ do not contribute.

6 Error covariance model

Spatial domain

The error covariance model in the spatial domain is modeled following *Daley* [1991]. The Gaussian model for the error covariances of the velocity potential and stream function in the spatial domain is defined as

$$f_{\psi}(r) = (1 - \nu^2)V_{\psi}e^{-r^2/R_{\psi}^2} , \quad (6.1a)$$

$$f_{\chi}(r) = \nu^2V_{\chi}e^{-r^2/R_{\chi}^2} , \quad (6.1b)$$

where ν^2 stands for the ratio of the rotational and the divergent contribution to the wind field, R_{ψ} and R_{χ} for the length scales determining the extent of the error correlations, and V_{ψ} and V_{χ} for the variance of the error in ψ and χ , respectively. The error covariance model presented above holds for isotropic errors in ψ and χ . The error variances V_{ψ} and V_{χ} are in the potential domain and therefore hard to estimate. It would be much more convenient to express them in the wind domain. The errors in the potential and wind domains are related as [*Daley*, 1991, section 5.2]

$$V_l = \frac{V_{\psi}}{L_{\psi}^2} , \quad V_t = \frac{V_{\chi}}{L_{\chi}^2} . \quad (6.2)$$

with V_l and V_t the variances of the error in the background wind components l and t , respectively. The scaling parameters L_{ψ} and L_{χ} are defined as

$$L_{\psi}^2 = -\frac{f_{\psi}(r)}{\nabla^2 f_{\psi}(r)} \Big|_{r=0} , \quad L_{\chi}^2 = -\frac{f_{\chi}(r)}{\nabla^2 f_{\chi}(r)} \Big|_{r=0} . \quad (6.3)$$

These relations are derived at the end of this chapter, since they are not explicitly given by *Daley*. Equation (6.3) holds for any form of the error correlation function. Note that *Daley* adds an additional factor of 2 in the right hand side of (6.3), but that is incorrect. For the Gaussian form (6.1) one readily finds

$$L_{\psi}^2 = \frac{1}{2}R_{\psi}^2 , \quad L_{\chi}^2 = \frac{1}{2}R_{\chi}^2 , \quad (6.4)$$


and (6.1) becomes

$$f_{\psi}(r) = (1 - \nu^2)V_l L_{\psi}^2 e^{-\frac{r^2}{R_{\psi}^2}} = \frac{1}{2}(1 - \nu^2)V_l R_{\psi}^2 e^{-\frac{r^2}{R_{\psi}^2}} , \quad (6.5a)$$

$$f_{\chi}(r) = \nu^2 V_t L_{\chi}^2 e^{-\frac{r^2}{R_{\chi}^2}} = \frac{1}{2}V_t R_{\chi}^2 e^{-\frac{r^2}{R_{\chi}^2}} . \quad (6.5b)$$

Frequency domain

Fourier transformation yields the error covariance model in the frequency domain. The Gaussian model will also be Gaussian in the frequency domain, see appendix G. Using equation (G.4) the error covariance in the frequency domain reads (see also 3.12)

<div style="display: flex; align-items: center;"> <div style="margin-right: 20px;"> <small>The EUMETSAT Network of Satellite Application Facilities</small> </div> <div>  NWP SAF <small>Numerical Weather Prediction</small> </div> </div>	<h2 style="margin: 0;">Two-dimensional variational ambiguity removal (2DVAR)</h2>	Doc ID : NWPSAF-KN-TR-004 Version : 1.6 Date : 13-08-2021
--	---	---

$$\hat{f}_{\psi}(p, q) = B_{\hat{\psi}\hat{\psi}}(p, q) = \frac{\pi}{2} (1 - \nu^2) V_l R_{\psi}^4 e^{-\pi^2 R_{\psi}^2 (p^2 + q^2)} \quad , \quad (6.6a)$$

$$\hat{f}_{\chi}(p, q) = B_{\hat{\chi}\hat{\chi}}(p, q) = \frac{\pi}{2} \nu^2 V_t R_{\chi}^4 e^{-\pi^2 R_{\chi}^2 (p^2 + q^2)} \quad . \quad (6.6b)$$

For the conditioning transformation we need the matrix elements of $B_{\hat{\psi}\hat{\psi}}^{1/2}$ and $B_{\hat{\chi}\hat{\chi}}^{1/2}$, which are the square root of (6.6)

$$B_{\hat{\psi}\hat{\psi}}^{1/2}(p, q) = \sqrt{\frac{\pi}{2} (1 - \nu^2)} \varepsilon_l R_{\psi}^2 e^{-\frac{1}{2} \pi^2 R_{\psi}^2 (p^2 + q^2)} \quad , \quad (6.7a)$$

$$B_{\hat{\chi}\hat{\chi}}^{1/2}(p, q) = \sqrt{\frac{\pi}{2}} \nu \varepsilon_t R_{\chi}^2 e^{-\frac{1}{2} \pi^2 R_{\chi}^2 (p^2 + q^2)} \quad , \quad (6.7b)$$

with $\varepsilon_l = \sqrt{V_l}$ and $\varepsilon_t = \sqrt{V_t}$.

Relation between errors in the wind domain and the potential domain

Daley [1991, section 5.2] defines the error covariances in the wind domain and in the potential domain as

$$C_{ll}(r) = E_l^2 \rho_{ll}(r) \quad , \quad C_{tt}(r) = E_t^2 \rho_{tt}(r) \quad , \quad (6.8a)$$

$$C_{\psi\psi}(r) = E_{\psi}^2 \rho_{\psi\psi}(r) \quad , \quad C_{\chi\chi}(r) = E_{\chi}^2 \rho_{\chi\chi}(r) \quad , \quad (6.8b)$$

where E^2 stands for the error variance and ρ for the error correlation. Comparison with the previous sections shows the correspondence $C \leftrightarrow f$ and $E^2 \leftrightarrow V$. Since $\rho(0) = 1$ it follows that for each component $C(0) = E^2$.

Daley also shows that in the isotropic case

$$C_{ll}(r) = -\frac{1}{r} \frac{d}{dr} C_{\psi\psi}(r) - \frac{d^2}{dr^2} C_{\chi\chi}(r) \quad , \quad (6.9a)$$

$$C_{tt}(r) = -\frac{1}{r} \frac{d}{dr} C_{\chi\chi}(r) - \frac{d^2}{dr^2} C_{\psi\psi}(r) \quad . \quad (6.9b)$$


Setting $r = 0$ lets the first derivatives vanish, since the covariances are symmetric functions of their argument.

The second derivatives evaluated at $r = 0$ can be written using (6.4) as

$$\left. \frac{d^2}{dr^2} C_{\psi\psi}(r) \right|_{r=0} = \nabla^2 C_{\psi\psi}(r) \Big|_{r=0} = -L_{\psi}^2 C_{\psi\psi}(0) \quad , \quad (6.10a)$$

$$\left. \frac{d^2}{dr^2} C_{\chi\chi}(r) \right|_{r=0} = \nabla^2 C_{\chi\chi}(r) \Big|_{r=0} = -L_{\chi}^2 C_{\chi\chi}(0) \quad . \quad (6.11b)$$

Substituting this in (6.9) and letting $C(0) = E^2$ immediately yields (6.5).

<div style="display: flex; align-items: center;"> <div style="margin-right: 20px;"> <small>The EUMETSAT Network of Satellite Application Facilities</small> </div> <div>  NWP SAF <small>Numerical Weather Prediction</small> </div> </div>	<h2 style="margin: 0;">Two-dimensional variational ambiguity removal (2DVAR)</h2>	Doc ID : NWPSAF-KN-TR-004 Version : 1.6 Date : 13-08-2021
--	---	---

7 Single observation test

Single observation solution

In case there is exactly one observation, the 2DVAR problem can be solved analytically. Suppose that at some point (x_i, y_j) on the 2DVAR grid there is one observation (u_o, v_o) with increment $(\delta u_o, \delta v_o)$. Starting with zero background increment and zero analysis increment field, the only contribution to the cost function and its gradient originates from this observation. From (4.9) and (4.10) this contribution reads

$$J_o = \frac{\delta u_o^2 + \delta v_o^2}{\varepsilon_o^2} = \frac{u_o^2 + v_o^2}{\varepsilon_o^2} \quad , \quad (7.1a)$$

$$\frac{\partial J_o}{\partial u_o} = \frac{2\delta u_o}{\varepsilon_o^2} = \frac{2u_o}{\varepsilon_o^2} \quad , \quad \frac{\partial J_o}{\partial v_o} = \frac{2\delta v_o}{\varepsilon_o^2} = \frac{2v_o}{\varepsilon_o^2} \quad . \quad (7.1b)$$

with $\varepsilon_o = \varepsilon_u = \varepsilon_v$. Now the 2DVAR problem reduces to an optimal interpolation problem [Daley, 1991] with solution

$$J_t^{\text{final}} = \frac{\varepsilon_B^2 \varepsilon_o^2}{(\varepsilon_B^2 + \varepsilon_o^2)^2} J_t^{\text{initial}} \quad , \quad (7.2)$$

where $J_t = J_o + J_b$ is the total cost function. At the solution point, the gradient of the total cost function should be zero, since the total cost function is minimal there. Therefore

$$\nabla J_b = -\nabla J_o \quad . \quad (7.3)$$

With these relations it is possible to calculate the final analysis field as shown schematically in figure 7.1. Starting with values for (u_o, v_o) and for ε_o and ε_B , the final cost function value is obtained from (7.2). The gradient of the observation part of the cost function is obtained from (7.1b). This yields the gradient of the background part of the cost function according to (7.3). Since the background cost function can be defined as $J_b = \xi^T \xi$, its gradient reads

$$\nabla J_b = 2\xi \quad . \quad (7.4)$$

From (7.4) the background potential field can be retrieved. See appendix E for a more elaborate derivation. The increment of the analysis wind equals the analysis wind itself, since the background is assumed to be zero, so at the observation point it satisfies

$$(u, v) = \frac{\varepsilon_B^2}{\varepsilon_B^2 + \varepsilon_o^2} (u_o, v_o) \quad . \quad (7.5)$$

Applying the unconditioning transformation to the background potential field yields the analysis wind field that should have the prescribed rotational and/or divergent structure determined by the value of ν set in the error covariance model. Since the wind speed at point (x_i, y_j) should satisfy (7.5), its value can be used to check the unconditioning transformation. A second check consists of packing the potential fields into a control vector and calculating the final background contribution to the total cost, which should satisfy (7.2), and that to the total gradient, which should satisfy (7.3).

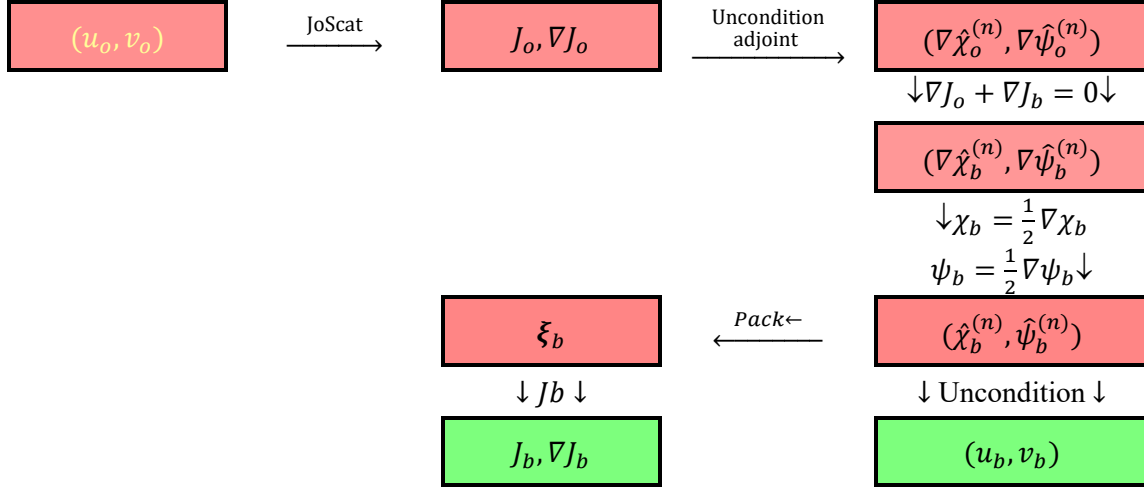


Figure 7.1 Scheme for calculating the solution in the single observation test. The green boxes indicate quantities that can be compared with the input values.

This test is implemented in program SOSC (Single Observation Solution Check). The required solution is retrieved within machine precision (about six decimal places).

Single Observation Analysis

The next step in testing the cost function and its gradient is to start with zero background and let 2DVAR's minimization routine find the solution. This is done in program SOAP (Single Observation Analysis Plot).

Figure 7.2 shows the resulting wind fields for (u_o, v_o) equal to (1,0) or (0,1) m/s and v equal to zero (purely rotational) or one (purely divergent). The observation is located in the centre of the grid, x and y equal to 1600 km. The range parameters R_ψ and R_χ are both equal to 300 km. The error variance in the observations and in the background field was set equal to $3.24 \text{ m}^2/\text{s}^2$ for both. The wind speed at x and y equal to 1600 km should equal half of the initial observation. This is satisfied with an accuracy better than $2 \cdot 10^{-5}$. The minimization in 2DVAR is performed by routine LBFGS [Liu and Nocedal, 1989]. The accuracy with which the solution is retrieved can be controlled with the parameter ε defined as

$$\varepsilon^2 = \frac{\|\nabla J_t\|}{\|J_t\|} = \frac{\sum_\lambda (\nabla J_t|_\lambda)^2}{\sum_\lambda J_t^2|_\lambda} \quad (7.7)$$

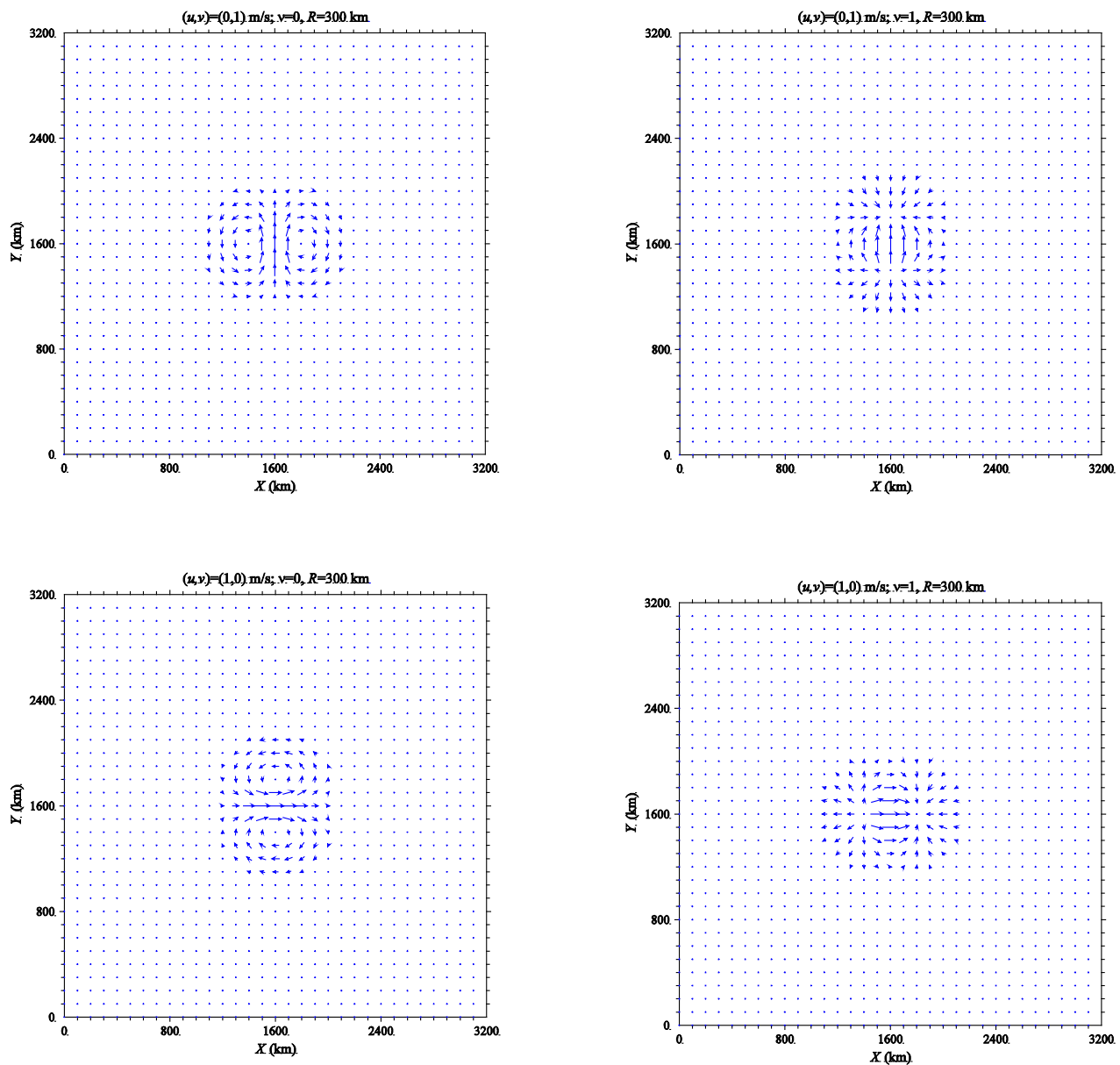


Figure 7.2 Results of the single observation test for various observations and values of the rotational/divergence ratio.

Iteration	J_t	$\frac{\ \nabla J_t\ }{\ J_t\ }$	v_c
1	0.308642		
2	0.30864152		
3	0.30863965		
4	0.30863214		
5	0.30860204		
6	0.3084817		
7	0.30800086		
8	0.30608514		
9	0.2985448		
10	0.2703461	$4.65 \cdot 10^{-12}$	0.06656095
11	0.15591854	$3.98 \cdot 10^{-14}$	0.49277255
12	0.15513143	$2.82 \cdot 10^{-14}$	0.49654663
13	0.15432084	$2.34 \cdot 10^{-19}$	0.5000003

Table 7.1 Convergence of 2DVAR's minimization in SOAP. The quantity v_c is the meridional wind speed at $x = y = 1600$ km and should equal 0.5 m/s.

Table 7.1 shows in detail the convergence of SOAP for $(u_o, v_o) = (0,1)$ m/s, $v = 0$ (purely rotational), and $R_\psi = R_\chi = 300$ km. The cost function does not converge with uniform speed. Convergence starts slowly but surely, with a rate of about one decimal place per iteration. The final solution is almost reached at the 11-th iteration. The last two iterations further improve the minimum.

Routine LBFGS stops when the calculated ratio of the norm of the cost gradient and the cost is smaller than ε . Table 7.1 shows that ε should be smaller than $4.65 \cdot 10^{-12}$, otherwise LBFGS would stop at iteration number 10 or earlier, before it has converged to a decent velocity field (v_c is much too small at iteration 10). On the other hand, ε should be larger than $2.34 \cdot 10^{-19}$, because otherwise LBFGS would be forced to search a minimum beyond machine precision. Therefore ε should be somewhere between 10^{-16} and 10^{-18} .

Positional properties

Figure 7.3 shows what happens with the single observation analysis when the observation is not in the centre of the 2DVAR grid (left panel), but at the edge (right panel). This figure was obtained with $(u_o, v_o) = (0,1)$ m/s, $v = 0$, and $R_\psi = R_\chi = 600$ km in order to extend the spatial range of the covariance structures. Figure 7.2 shows that the analysis is periodic. In order to prevent mixing of observations at the grid edges, the 2DVAR grid should be extended such that the periodicity of the analysis has no influence on the final 2DVAR results. The size of such an extension depends on the spatial scale of the background error correlation lengths R_ψ and R_χ . It should be several times the correlation length.

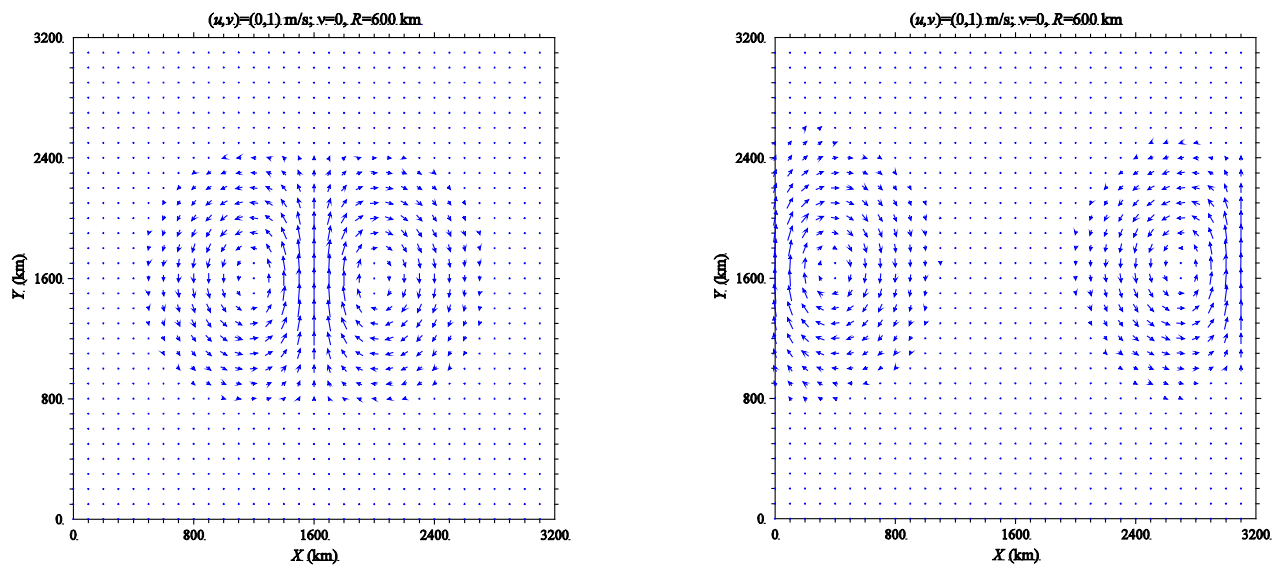





Figure 7.2 Effect of the observation position on the analysis.

<p>The EUMETSAT Network of Satellite Application Facilities</p> 	<h1>Two-dimensional variational ambiguity removal (2DVAR)</h1>	<p>Doc ID : NWPSAF-KN-TR-004 Version : 1.6 Date : 13-08-2021</p>
---	--	--

 	Two-dimensional variational ambiguity removal (2DVAR)	Doc ID : NWPSAF-KN-TR-004 Version : 1.6 Date : 13-08-2021
---	--	---

8 Some implementation notes

Evaluation of the cost function and its gradient

The background contribution to the cost function reads

$$J_b = 2 \int_{-\infty}^{\infty} dp \int_0^{\infty} dq \xi^2 \approx \Delta p \Delta q \sum_{\lambda=1}^{2(N_1 N_2 - 1)} w_{\lambda} \xi_{\lambda}^2, \quad (8.1)$$

where the integral has been approximated by the sum over the gridded potential fields normalized with the integration weight $\Delta p \Delta q = (N_1 N_2 \Delta^2)^{-1}$, Δ being the 2DVAR grid size in position space.


The following points must be noted:

- It is not necessary to use a higher order approximation for the integral like Simpson's rule, because the Fourier transforms are evaluated at the same order.
- Since the observation part of the cost function is evaluated in position space, the integration weight in (8.1) must be included. Otherwise the two components of the cost function differ in normalization and can not be added to yield the total cost.
- The control vector weights in (8.1) reflect the fact that the potential fields are Hermitian. They should be applied not only to J_b , but also to its gradient ∇J_b and to the gradient of the observation cost, ∇J_o . This is because the potential fields due to the observations are also Hermitian.
- The present implementation of 2DVAR uses complex matrices of dimension $N_1 \times N_2$ in the frequency domain and a complex-to-complex FFT routine. Since the potential fields are Hermitian, it is not necessary to calculate the transformation and the convolution (or their adjoints) for all indices $i_1 = 1, \dots, N_1$ and $i_2 = 1, \dots, N_2$. It would be sufficient to take only the independent components into account. A simple method with slight overhead would be to limit the index i_2 to non-negative frequencies only, $i_2 = 1, \dots, k_2$ with $k_2 = \frac{1}{2} N_2 + 1$. Such an adaptation in combination with a real-to-real FFT routine would increase the computational efficiency of 2DVAR – at the cost of more complicated code. Since 2DVAR in its present form is fast enough to meet all operational requirements so far, this adaptation has low priority.

The backward FFT in genscat support is defined as (see appendix A)

$$u_{k,l} = \frac{1}{N_1 N_2} \sum_{m=0}^{N_1-1} \sum_{n=0}^{N_2-1} \hat{u}_{m,n} e^{-2\pi i \left(\frac{km}{N_1} + \frac{ln}{N_2} \right)}, \quad (8.2)$$

i.e., including a normalization factor $(N_1 N_2)^{-1}$ and therefore assuming unity grid size. The adjoint of (8.2) is simply the forward FFT and should contain the proper normalization factor Δ^2 , with Δ the 2DVAR grid size. Because the factor $(N_1 N_2)^{-1}$ is included in the lowest level FFT routine, the adjoint inverse FFT routine in genscat still contains the normalization factor $(N_1 N_2)^{-1}$ if it is defined as the complex conjugate of the inverse FFT.

<div data-bbox="140 129 255 185"> The EUMETSAT Network of Satellite Application Facilities </div> <div data-bbox="284 136 550 212">  NWP SAF Numerical Weather Prediction </div>	Two-dimensional variational ambiguity removal (2DVAR)	Doc ID : NWPSAF-KN-TR-004 Version : 1.6 Date : 13-08-2021
---	--	---

- In order to avoid confusion regarding the normalizations in the forward and inverse FFT routines, it is better to use a forward FFT routine rather than an adjoint inverse routine in 2DVAR.

Initial minimization step size

The minimization is performed by routine LBFGS [*Liu and Nocedal, 1989*]. The size of the first step is estimated in the original routine as $1/|g(0)|$, where $g(0)$ is the gradient at the initial point $\xi = 0$. This step size may be much too small for 2DVAR, causing the minimization procedure to get stuck at the first point. It is shown in appendix H that for the 2DVAR problem a better first step size is given by $f(0)/|g(0)|$, with $f(0)$ the value of the cost function at the initial point.

In practice, a first step size of $30f(0)/|g(0)|$ leads to some improvement, because on average less function evaluations are needed to find the minimum.

9 Resume

The relevant formulas for 2DVAR are collected in this paragraph. The analysis wind field is found by minimizing a cost function $J(\xi)$ expressed in terms of the so-called preconditioned control vector ξ which is expressed in terms of the normalized potential fields in the frequency domain. If δx stands for the control vector in terms of the analysis increments in the spatial domain, it is related to ξ by the unconditioning transformation

$$\delta x = U \xi \quad . \quad (9.1)$$

The cost function is given by

$$J = J_b + J_o \quad , \quad (9.2)$$

with the background term J_b expressed in terms of the normalized potential fields in the frequency domain as

$$J_b = \sum_{\lambda=1}^{2(N_1 N_2 - 1)} w_{\lambda} \xi_{\lambda}^T \xi_{\lambda} \quad , \quad (9.3)$$

where the index λ runs over all independent potential field components, and the weights w are determined by the fact that the potential fields are Hermitian on one hand, and the properties of the FFT algorithm on the other. The observation term J_o in terms of the analysis increments in the spatial domain reads

$$J_o = \sum_{m=1}^{N_{obs}} J_s^{-1/p} \quad , \quad (9.4a)$$

$$J_s = \sum_{k=1}^{M_m} \left(\frac{(\delta \bar{t}_m - \delta t_{m,k}^{(o)})^2}{\varepsilon_t^2} + \frac{(\delta \bar{l}_m - \delta l_{m,k}^{(o)})^2}{\varepsilon_l^2} - 2 \ln P_k \right)^{-p} \quad , \quad (9.4b)$$

where the analysis increments $\delta \bar{t}_m$ and $\delta \bar{l}_m$ are interpolated from the 2DVAR analysis grid to the position of observation m . In (9.4) we have $p = 4$ and $\varepsilon_t = \varepsilon_l = 1.8 \text{m/s}$. Note that t stands for the transversal wind component in the 2DVAR batch grid and l for the longitudinal one.

The contribution of the background term to component λ of the cost function gradient reads

$$\nabla J_b|_{\lambda} = 2 w_{\lambda} \xi_{\lambda} \quad . \quad (9.5)$$


The derivatives of the observation part of the cost function in the positional domain read

$$\frac{\partial J_o}{\partial \delta \bar{t}_m} = \frac{\partial J_o}{\partial J_s} \frac{\partial J_s}{\partial \delta \bar{t}_m} = \frac{-1}{p} J_s^{-1-\frac{1}{p}} \frac{\partial J_s}{\partial \delta \bar{t}_m} \quad , \quad (9.6a)$$

$$\frac{\partial J_o}{\partial \delta \bar{l}_m} = \frac{\partial J_o}{\partial J_s} \frac{\partial J_s}{\partial \delta \bar{l}_m} = \frac{-1}{p} J_s^{-1-1/p} \frac{\partial J_s}{\partial \delta \bar{l}_m} \quad , \quad (9.6b)$$

with

$$\frac{\partial J_s}{\partial \delta \bar{t}_m} = -p \sum_{k=1}^{M_m} \left(\frac{(\delta \bar{t}_m - \delta t_{m,k}^{(o)})^2}{\varepsilon_t^2} + \frac{(\delta \bar{l}_m - \delta l_{m,k}^{(o)})^2}{\varepsilon_l^2} - 2 \ln P_k \right)^{-p-1} \frac{2(\delta \bar{t}_m - \delta t_{m,k}^{(o)})}{\varepsilon_t^2} \quad , \quad (9.7a)$$

<div style="display: flex; align-items: center;"> <div style="margin-right: 20px;"> <small>The EUMETSAT Network of Satellite Application Facilities</small> </div> <div>  NWP SAF <small>Numerical Weather Prediction</small> </div> </div>	<h2 style="margin: 0;">Two-dimensional variational ambiguity removal (2DVAR)</h2>	<div style="font-family: monospace;"> Doc ID : NWPSAF-KN-TR-004 Version : 1.6 Date : 13-08-2021 </div>
--	---	--

$$\frac{\partial J_s}{\partial \bar{l}_m} = -p \sum_{k=1}^{M_m} \left(\frac{(\delta \bar{t}_m - \delta t_{m,k}^{(o)})^2}{\varepsilon_t^2} + \frac{(\delta \bar{l}_m - \delta l_{m,k}^{(o)})^2}{\varepsilon_l^2} - 2 \ln P_k \right)^{-p-1} \frac{2(\delta \bar{l}_m - \delta l_{m,k}^{(o)})}{\varepsilon_l^2} . \quad (9.7b)$$

As stated before, the spatial domain and the frequency domain are connected by the unconditioning transformation (9.1). The gradient of the observation part of the cost function in the frequency domain is given by

$$\nabla_{\xi} J_o = \mathbf{U}^* \nabla_x J_o , \quad (9.8)$$

where \mathbf{U}^* is the adjoint of \mathbf{U} (i.e., the complex conjugate of its transpose) and the gradient vector $\nabla_x J_o$ has the derivatives (9.6) as its components, the subscripts of the gradient operators indicating the domain.

The unconditioning transformation consists of three parts,

$$\mathbf{U} = \mathbf{B}_{\hat{\chi}, \hat{\psi}}^{1/2} \mathbf{H} \mathbf{F}^{-1} , \quad (9.9)$$

with \mathbf{F}^{-1} the inverse Fourier transform, \mathbf{H} the Helmholtz transformation operator, and $\mathbf{B}_{\hat{\chi}, \hat{\psi}}^{1/2}$ the square root of the factorized background error covariance matrix expressed in terms of stream function and wind potential in wavenumber space.

The discrete inverse Fourier transform reads

$$t_{k,l} = \frac{1}{N_1 N_2 \Delta^2} \sum_{m=0}^{N_1-1} \sum_{n=0}^{N_2-1} \hat{t}_{m,n} e^{-2\pi i \left(\frac{km}{N_1} + \frac{ln}{N_2} \right)} , \quad (9.10a)$$

$$l_{k,l} = \frac{1}{N_1 N_2 \Delta^2} \sum_{m=0}^{N_1-1} \sum_{n=0}^{N_2-1} \hat{l}_{m,n} e^{-2\pi i \left(\frac{km}{N_1} + \frac{ln}{N_2} \right)} , \quad (9.10b)$$

where Δ is the size of the spatial grid that has dimensions $N_1 \times N_2$.

The Helmholtz transformation is given by

$$\hat{t} = \hat{h}_1 \hat{\chi} - \hat{h}_2 \hat{\psi} , \quad (9.11a)$$

$$\hat{l} = \hat{h}_2 \hat{\chi} + \hat{h}_1 \hat{\psi} , \quad (9.11b)$$

with

$$\hat{h}_1(p) = -2\pi i p , \quad (9.12a)$$

$$\hat{h}_2(q) = -2\pi i q . \quad (9.12b)$$


The normalization reads

$$B_{\hat{\psi}\hat{\psi}}^{1/2}(p, q) = \left[\iint dx dy f_{\psi}(x, y) e^{2\pi i(p x + q y)} \right]^{\frac{1}{2}} , \quad (9.13a)$$

$$B_{\hat{\chi}\hat{\chi}}^{1/2}(p, q) = \left[\iint dx dy f_{\chi}(x, y) e^{2\pi i(p x + q y)} \right]^{\frac{1}{2}} . \quad (9.13b)$$

The error correlation function in the spatial domain are defined as a function of $r = \sqrt{x^2 + y^2}$ as

$$f_{\psi}(r) = (1 - \nu^2) V_l L_{\psi}^2 e^{-\frac{r^2}{R_{\psi}^2}} , \quad (9.14a)$$


<div data-bbox="140 129 255 183" data-label="Page-Header"> <p>The EUMETSAT Network of Satellite Application Facilities</p> </div> <div data-bbox="284 138 550 210" data-label="Page-Header">  <p>NWP SAF Numerical Weather Prediction</p> </div>	<p>Two-dimensional variational ambiguity removal (2DVAR)</p>	<p>Doc ID : NWPSAF-KN-TR-004 Version : 1.6 Date : 13-08-2021</p>
--	--	--

$$f_{\chi}(r) = v^2 V_t L_{\chi}^2 e^{-r^2/R_{\chi}^2} , \quad (9.14b)$$

where V_l and V_t stand for the variance of the error in l and t , respectively, and v^2 for the ratio of the rotational and the divergent contribution to the wind field. The length scales R_{ψ} and R_{χ} determine the extent of the error correlations, and the scaling parameters L_{ψ} and L_{χ} for the transformation of the error variances from the potential domain to the wind domain are defined as

$$L_{\psi}^2 = -\frac{2f_{\psi}(r)}{v^2 f_{\psi}(r)} \Big|_{r=0} , \quad L_{\chi}^2 = -\frac{2f_{\chi}(r)}{v^2 f_{\chi}(r)} \Big|_{r=0} . \quad (9.15)$$

For Gaussian error covariances the normalizations can be calculated analytically.

<p>The EUMETSAT Network of Satellite Application Facilities</p> 	<h1>Two-dimensional variational ambiguity removal (2DVAR)</h1>	<p>Doc ID : NWPSAF-KN-TR-004 Version : 1.6 Date : 13-08-2021</p>
---	--	--

10 Flow dependent background errors

In the preceding chapters it was assumed that the background error covariance matrix \mathbf{B} (or, more precisely, its inverse) was a function of the distance between two points only, and that the background error variances were constant within a batch. It will now first be shown that this considerably simplifies evaluation of the background cost function when transformed to wavenumber space. If the background errors are flow dependent, they are no longer constant but depend on position. It will be shown that this can easily be incorporated in the current 2DVAR scheme.

General case

In position space, the background cost function can be written in continuous representation as (c.f. equation (2.10))

$$J_b = \int d\mathbf{x} \int d\mathbf{x}' \delta^*(\mathbf{x}) \mathbf{B}^{-1}(\mathbf{x}, \mathbf{x}') \delta(\mathbf{x}') \quad , \quad (10.1)$$

where $\mathbf{x} = (x, y)$, $\mathbf{x}' = (x', y')$, and δ stands for δu or δv . This is the usual expression for a scalar product in Hilbert space. The star indicating complex conjugation could be omitted in (10.1) since δ is a real vector. However, it is useful to keep it as a reminder for the case δ is Fourier transformed. Transforming to wavenumber space, the cost function reads

$$J_b = \int d\mathbf{x} \int d\mathbf{x}' \int d\mathbf{p} e^{2\pi i \mathbf{p} \cdot \mathbf{x}} \hat{\delta}^*(\mathbf{p}) \int d\mathbf{q} \int d\mathbf{q}' e^{-2\pi i \mathbf{q} \cdot \mathbf{x}} e^{-2\pi i \mathbf{q}' \cdot \mathbf{x}'} \hat{\mathbf{B}}^{-1}(\mathbf{q}, \mathbf{q}') \times \\ \times \int d\mathbf{p}' e^{-2\pi i \mathbf{p}' \cdot \mathbf{x}'} \hat{\delta}(\mathbf{p}') \quad . \quad (10.2)$$

Rearranging terms yields

$$J_b = \int d\mathbf{p} \int d\mathbf{q} \int d\mathbf{q}' \int d\mathbf{p}' \hat{\delta}^*(\mathbf{p}) \hat{\mathbf{B}}^{-1}(\mathbf{q}, \mathbf{q}') \hat{\delta}(\mathbf{p}') \int d\mathbf{x} e^{-2\pi i (\mathbf{q} - \mathbf{p}) \cdot \mathbf{x}} \int d\mathbf{x}' e^{-2\pi i (\mathbf{p}' + \mathbf{q}') \cdot \mathbf{x}'} \quad . \quad (10.3)$$

The integrals over position yield delta functions, so

$$J_b = \int d\mathbf{p} \int d\mathbf{p}' \hat{\delta}^*(\mathbf{p}) \hat{\mathbf{B}}^{-1}(\mathbf{p}, -\mathbf{p}') \hat{\delta}(-\mathbf{p}') \quad . \quad (10.4)$$

Since \mathbf{B} and δ are real functions in position space, their Fourier transforms are symmetric in their arguments, and therefore

$$J_b = \int d\mathbf{p} \int d\mathbf{p}' \hat{\delta}^*(\mathbf{p}) \hat{\mathbf{B}}^{-1}(\mathbf{p}, \mathbf{p}') \hat{\delta}(\mathbf{p}') \quad . \quad (10.5)$$

Now the evaluation of J_b in wavenumber space requires as many integrations as in position space, so transformation to wavenumber space yields no gain in efficiency for evaluating J_b .

Constant background errors

In the preceding chapter it was assumed that the background error variances were constant (at least within a batch), and that the background error correlation was a function of distance. This can be expressed as $\mathbf{B}^{-1} = \mathbf{B}^{-1}(\mathbf{x} - \mathbf{x}')$, so

$$J_b = \int d\mathbf{x} \int d\mathbf{x}' \delta^*(\mathbf{x}) \mathbf{B}^{-1}(\mathbf{x} - \mathbf{x}') \delta(\mathbf{x}') \quad , \quad (10.6)$$

Taking Fourier transforms, one arrives at

$$J_b = \int d\mathbf{x} \int d\mathbf{x}' \int d\mathbf{p} e^{2\pi i \mathbf{p} \cdot \mathbf{x}} \hat{\delta}^*(\mathbf{p}) \int d\mathbf{q} e^{-2\pi i \mathbf{q} \cdot (\mathbf{x} - \mathbf{x}')} \hat{\mathbf{B}}^{-1}(\mathbf{q}) \int d\mathbf{p}' e^{-2\pi i \mathbf{p}' \cdot \mathbf{x}'} \hat{\delta}(\mathbf{p}') \quad . \quad (10.7)$$

Rearranging terms yields

$$J_b = \int d\mathbf{p} \int d\mathbf{q} \int d\mathbf{p}' \hat{\delta}^*(\mathbf{p}) \hat{\mathbf{B}}^{-1}(\mathbf{q}) \hat{\delta}(\mathbf{p}') \int d\mathbf{x} e^{-2\pi i (\mathbf{p} - \mathbf{q}) \cdot \mathbf{x}} \int d\mathbf{x}' e^{-2\pi i (\mathbf{q} - \mathbf{p}') \cdot \mathbf{x}'} \quad . \quad (10.8)$$

The integrals over \mathbf{x} and \mathbf{x}' give delta functions $\delta(\mathbf{p} - \mathbf{q})$ and $\delta(\mathbf{q} - \mathbf{p}')$, respectively, so

$$J_b = \int d\mathbf{p} \hat{\delta}^*(\mathbf{p}) \hat{\mathbf{B}}^{-1}(\mathbf{p}) \hat{\delta}(\mathbf{p}) \quad . \quad (10.9)$$

Note that evaluation of J_b in wavenumber space now requires a single two-dimensional integration, whereas its evaluation in position space according to (10.6) requires a double two-dimensional integral. Therefore J_b is calculated much more efficient in wavenumber space than in position space if the background error variances are constant and the background error correlations are a function of distance only. In fact, the number of integrations could be reduced even further when going to polar coordinates, since actually $\mathbf{B}^{-1} = \mathbf{B}^{-1}(|\mathbf{x} - \mathbf{x}'|)$. This, however, would lead to some implementational problems since the FFT algorithm used for the Fourier transforms is restricted to Cartesian coordinates.

Flow dependent background errors

The case of flow dependent background errors (background errors that vary with position) while the background error correlation is a function of distance (so the shape of the background error covariance is constant) is in fact quite simple. The background covariance matrix can be factored as $\mathbf{B}(\mathbf{x}, \mathbf{x}') = \mathbf{\Sigma}(\mathbf{x}) \mathbf{\Gamma}(\mathbf{x} - \mathbf{x}') \mathbf{\Sigma}(\mathbf{x}')$, see (3.13). Since \mathbf{B} is symmetric in its arguments, one can write

$$\mathbf{B}^{-1}(\mathbf{x}, \mathbf{x}') = \mathbf{B}^{-1}(\mathbf{x}', \mathbf{x}) = \mathbf{\Sigma}^{-1}(\mathbf{x}) \mathbf{\Gamma}^{-1}(\mathbf{x} - \mathbf{x}') \mathbf{\Sigma}^{-1}(\mathbf{x}') \quad . \quad (10.10)$$

Substituting this in (10.1) yields

$$J_b = \int d\mathbf{x} \int d\mathbf{x}' \hat{\delta}^*(\mathbf{x}) \mathbf{\Sigma}^{-1}(\mathbf{x}) \mathbf{\Gamma}^{-1}(\mathbf{x} - \mathbf{x}') \mathbf{\Sigma}^{-1}(\mathbf{x}') \hat{\delta}(\mathbf{x}') \quad . \quad (10.11)$$


Putting $\Delta(\mathbf{x}) = \mathbf{\Sigma}^{-1}(\mathbf{x}) \hat{\delta}(\mathbf{x})$, so $\Delta^*(\mathbf{x}) = (\mathbf{\Sigma}^{-1}(\mathbf{x}) \hat{\delta}(\mathbf{x}))^* = \hat{\delta}^*(\mathbf{x}) \mathbf{\Sigma}^{-1}(\mathbf{x})$ since $\mathbf{\Sigma}$ is real, and substituting in (10.11) results in

$$J_b = \int d\mathbf{x} \int d\mathbf{x}' \Delta^*(\mathbf{x}) \mathbf{\Gamma}^{-1}(\mathbf{x} - \mathbf{x}') \Delta(\mathbf{x}') \quad . \quad (10.12)$$


This is the same as (10.6) with $\delta \rightarrow \Delta$ and $\mathbf{B} \rightarrow \mathbf{\Gamma}$. Repeating the Fourier transformations (10.7) and (10.8) immediately yields the final result



$$J_b = \int d\mathbf{p} \hat{\Delta}^*(\mathbf{p}) \hat{\mathbf{\Gamma}}^{-1}(\mathbf{p}) \hat{\Delta}(\mathbf{p}) \quad . \quad (10.13)$$

This shows that implementation of position dependent background errors in 2DVAR is very simple: the background covariance matrix must be replaced by the background error correlation matrix, and the velocity increments must be multiplied by the standard deviation of the background error.

<div data-bbox="140 129 255 185"> The EUMETSAT Network of Satellite Application Facilities </div> <div data-bbox="284 138 550 212">  NWP SAF Numerical Weather Prediction </div>	<h1>Two-dimensional variational ambiguity removal (2DVAR)</h1>	Doc ID : NWPSAF-KN-TR-004 Version : 1.6 Date : 13-08-2021
--	--	---

Flow dependent background errors may be obtained from the ECMWF Ensemble Data Assimilation system [Bonavita *et al.*, 2012] or from the scatterometer data itself using MLE and singularity exponents [Lin *et al.*, 2016].

<p>The EUMETSAT Network of Satellite Application Facilities</p> 	<h1>Two-dimensional variational ambiguity removal (2DVAR)</h1>	<p>Doc ID : NWPSAF-KN-TR-004 Version : 1.6 Date : 13-08-2021</p>
---	--	--

 	Two-dimensional variational ambiguity removal (2DVAR)	Doc ID : NWPSAF-KN-TR-004 Version : 1.6 Date : 13-08-2021
---	--	---

Appendix A Fourier transformation

Continuous case

Suppose the two-dimensional surface wind field \mathbf{v} in the spatial domain is a continuous function of the horizontal coordinates x and y , $\mathbf{v} = (u(x, y), v(x, y))$. Define the Fourier transforms \hat{u} and \hat{v} according to [Press *et al.*, 1988]

$$\hat{u}(p, q) = F[u](p, q) = \iint dx dy u(x, y) e^{2\pi i(px+qy)} , \quad (\text{A.1a})$$

$$\hat{v}(p, q) = F[v](p, q) = \iint dx dy v(x, y) e^{2\pi i(px+qy)} , \quad (\text{A.1b})$$

with p and q spatial frequencies, and the integration extending over the whole real axis. The hats indicate functions that are defined in the frequency domain; the square brackets indicate the argument of an operator. Note that p and q are spatial frequencies and not spatial wave numbers, because of the definition of the exponential in the Fourier transform. The inverse transform reads

$$u(x, y) = F^{-1}[\hat{u}](x, y) = \iint dp dq \hat{u}(p, q) e^{-2\pi i(px+qy)} , \quad (\text{A.2a})$$

$$v(x, y) = F^{-1}[\hat{v}](x, y) = \iint dp dq \hat{v}(p, q) e^{-2\pi i(px+qy)} . \quad (\text{A.2b})$$

This can be easily shown by substituting (A.1a) in (A.2a) and (A.1b) in (A.2b) and using

$$\int dp e^{2\pi i p(x-x')} = \delta(x - x') , \quad (\text{A.3})$$

the function on the right hand side of (A.3) being the Dirac delta function. Note that no normalization constant is involved, because it is included as the factor 2π in the exponentials.

Discrete case

The discrete 2D Fourier transform on a position grid with grid size Δ reads (see, e.g., Press *et al.*, [1988])

$$\hat{u}_{m,n} = \Delta^2 \sum_{k=0}^{M-1} \sum_{l=0}^{N-1} u_{k,l} e^{2\pi i \left(\frac{km}{M} + \frac{ln}{N} \right)} , \quad (\text{A.4})$$


where $u_{k,l} = u(x_k, y_l)$ with $x_k = k\Delta$ and $y_l = l\Delta$, k running from 0 to $N - 1$ and l from 0 to $M - 1$. The summation in the right hand side of (A.4) is performed by a FFT algorithm. The normalization factor Δ^2 has to be added explicitly in the 2DVAR software.

The inverse discrete 2D Fourier transform reads

$$u_{k,l} = \frac{1}{NM\Delta^2} \sum_{m=0}^{M-1} \sum_{n=0}^{N-1} \hat{u}_{m,n} e^{-2\pi i \left(\frac{km}{M} + \frac{ln}{N} \right)} , \quad (\text{A.5})$$

which is shown easily to hold by substitution of (A.4) in (A.5) or vice versa. As with the forward transform, the normalization factor in front of the summation is not set by the FFT algorithm, so it has to be included explicitly in the 2DVAR code.

Note that the normalization factor of the forward discrete transform equals the product of the grid sizes in the spatial domain, $\Delta^2 = \Delta_x \Delta_y$, while the normalization factor of the inverse discrete transform equals the product

<div data-bbox="140 129 256 185"> The EUMETSAT Network of Satellite Application Facilities </div> <div data-bbox="284 138 550 212">  NWP SAF Numerical Weather Prediction </div>	<h1>Two-dimensional variational ambiguity removal (2DVAR)</h1>	Doc ID : NWPSAF-KN-TR-004 Version : 1.6 Date : 13-08-2021
---	--	---

of the grid sizes in the frequency domain, $(N\Delta)^{-1}(M\Delta)^{-1} = \Delta p \Delta q$. With these definitions, the summations are easily recognized as the corresponding integrals evaluated with the simple first-order formula (left Riemann sum)

$$\int_a^b dx f(x) \approx \Delta \sum_{n=0}^{N-1} f(x_n) \quad , \quad (\text{A.6})$$

with $x_0 = a$, $x_N = b$, and

$$\Delta = \frac{b-a}{N} \quad . \quad (\text{A.7})$$

Appendix B Helmholtz transformation

Continuous boundary conditions

The operator $\mathbf{H} = (H_1, H_2)$ is in the spatial domain defined as

$$u(x, y) = H_1[\chi, \psi](x, y) = \frac{\partial \chi(x, y)}{\partial x} - \frac{\partial \psi(x, y)}{\partial y} , \quad (\text{B.1a})$$

$$v(x, y) = H_2[\chi, \psi](x, y) = \frac{\partial \chi(x, y)}{\partial y} + \frac{\partial \psi(x, y)}{\partial x} , \quad (\text{B.1b})$$

with χ the velocity potential and ψ the stream function. The inverse operator $\mathbf{H}^{-1} = (H_1^{-1}, H_2^{-1})$ satisfies

$$\chi(x, y) = H_1^{-1}[u, v](x, y) , \quad (\text{B.2a})$$

$$\psi(x, y) = H_2^{-1}[u, v](x, y) . \quad (\text{B.2b})$$

The explicit form of the operator and its inverse is more easily evaluated in the frequency domain., especially for numerical applications.

From (B.2a) and (A.2a) it follows that

$$\begin{aligned} u(x, y) &= H_1[\chi, \psi](x, y) = H_1 \left[F^{-1}[\hat{\chi}], F^{-1}[\hat{\psi}] \right] (x, y) = \\ &= \frac{\partial F^{-1}[\hat{\chi}](x, y)}{\partial x} - \frac{\partial F^{-1}[\hat{\psi}](x, y)}{\partial y} = \\ &= \frac{\partial}{\partial x} \int dp dq \hat{\chi}(p, q) e^{-2\pi i(px+qy)} - \frac{\partial}{\partial y} \int dp dq \hat{\psi}(p, q) e^{-2\pi i(px+qy)} . \end{aligned}$$

Note that the arguments of the functions in the frequency domain have been omitted at some places to keep the equations readable. The order of differentiation and integration may be interchanged for well behaving functions, so

$$\begin{aligned} u(x, y) &= \int dp dq (-2\pi i p) \hat{\chi}(p, q) e^{-2\pi i(px+qy)} - \int dp dq (-2\pi i q) \hat{\psi}(p, q) e^{-2\pi i(px+qy)} = \\ &= \int dp dq \hat{h}_1(p, q) \hat{\chi}(p, q) e^{-2\pi i(px+qy)} - \int dp dq \hat{h}_2(p, q) \hat{\psi}(p, q) e^{-2\pi i(px+qy)} = \\ &= F^{-1}[\hat{h}_1 \hat{\chi}](x, y) - F^{-1}[\hat{h}_2 \hat{\psi}](x, y) , \end{aligned}$$

with


$$\begin{aligned} \hat{h}_1(p, q) &= -2\pi i p , \\ \hat{h}_2(p, q) &= -2\pi i q . \end{aligned} \quad (\text{B.3})$$

From the previous equations one finds in the spatial domain, dropping the arguments of all functions

$$H_1[F^{-1}[\hat{\chi}], F^{-1}[\hat{\psi}]] = F^{-1}[\hat{h}_1 \hat{\chi}] - F^{-1}[\hat{h}_2 \hat{\psi}] . \quad (\text{B.4})$$

In the same way one obtains

$$v(x, y) = H_2[\chi, \psi](x, y) = H_2 \left[F^{-1}[\hat{\chi}], F^{-1}[\hat{\psi}] \right] (x, y) =$$

<div style="display: flex; align-items: center;"> <div style="margin-right: 20px;"> <small>The EUMETSAT Network of Satellite Application Facilities</small> </div> <div>  NWP SAF <small>Numerical Weather Prediction</small> </div> </div>	<h2 style="margin: 0;">Two-dimensional variational ambiguity removal (2DVAR)</h2>	<div style="font-family: monospace;"> Doc ID : NWPSAF-KN-TR-004 Version : 1.6 Date : 13-08-2021 </div>
--	---	--

$$\begin{aligned}
&= \frac{\partial F^{-1}[\hat{\chi}](x, y)}{\partial y} + \frac{\partial F^{-1}[\hat{\psi}](x, y)}{\partial x} = \\
&= \frac{\partial}{\partial y} dpdq \hat{\chi}(p, q) e^{-2\pi i(px+qy)} + \frac{\partial}{\partial x} dpdq \hat{\psi}(p, q) e^{-2\pi i(px+qy)} = \\
&= dpdq (-2\pi i q) \hat{\chi}(p, q) e^{-2\pi i(px+qy)} + dpdq (-2\pi i p) \hat{\psi}(p, q) e^{-2\pi i(px+qy)} = \\
&= dpdq \hat{h}_2(p, q) \hat{\chi}(p, q) e^{-2\pi i(px+qy)} + dpdq \hat{h}_1(p, q) \hat{\psi}(p, q) e^{-2\pi i(px+qy)} = \\
&= F^{-1}[\hat{h}_2 \hat{\chi}](x, y) + F^{-1}[\hat{h}_1 \hat{\psi}](x, y) \quad .
\end{aligned}$$

So, again dropping the arguments of the functions

$$H_2[F^{-1}[\hat{\chi}], F^{-1}[\hat{\psi}]] = F^{-1}[\hat{h}_2 \hat{\chi}] + F^{-1}[\hat{h}_1 \hat{\psi}] \quad . \quad (\text{B.5})$$

In what follows the function arguments are dropped when possible. For functions in the spatial domain the arguments are assumed to be (x, y) , and for functions in the frequency domain (p, q) , unless explicitly stated otherwise.

Using the fact that the inverse Fourier operator is linear, (B.4) can be cast into the form

$$u = F^{-1}[\hat{h}_1 \hat{\chi} - \hat{h}_2 \hat{\psi}] \quad .$$

Applying a Fourier transformation to both sides yields in the frequency domain

$$\hat{u} = \hat{h}_1 \hat{\chi} - \hat{h}_2 \hat{\psi} \quad . \quad (\text{B.6a})$$

Along the same lines one obtains

$$\hat{v} = \hat{h}_2 \hat{\chi} + \hat{h}_1 \hat{\psi} \quad . \quad (\text{B.6b})$$

Equation (B.6) shows that the Helmholtz operator is a simple linear transformation in the frequency domain. Its inverse is easily found by solving (B.6) for $\hat{\chi}$ and $\hat{\psi}$. This yields

$$\hat{\chi} = \hat{h}_1^{-1} \hat{u} + \hat{h}_2^{-1} \hat{v} \quad , \quad (\text{B.7a})$$

$$\hat{\psi} = -\hat{h}_2^{-1} \hat{u} + \hat{h}_1^{-1} \hat{v} \quad , \quad (\text{B.7b})$$

with



$$\hat{h}_1^{-1}(p, q) = \frac{i}{2\pi} \frac{p}{p^2 + q^2} \quad , \quad (\text{B.8a})$$

$$\hat{h}_2^{-1}(p, q) = \frac{i}{2\pi} \frac{q}{p^2 + q^2} \quad . \quad (\text{B.8b})$$

These equations are easily discretized for application on the 2DVAR grid.

Periodic boundary conditions

De Vries et al. derive the Helmholtz transformation equations on a discrete grid, since in 2DVAR the wind speed components and the potentials are evaluated on discrete grids. Their derivation is repeated below, and their results differ from those obtained in the preceding paragraph. This is because they implicitly assume

 	<h1>Two-dimensional variational ambiguity removal (2DVAR)</h1>	Doc ID : NWPSAF-KN-TR-004 Version : 1.6 Date : 13-08-2021
---	--	---

periodic boundary conditions: the equations are discretized and evaluated on a finite grid, whereas in the previous paragraph the equations were evaluated in infinite space and discretized afterwards.

The forward Helmholtz transformation in the formulation of *De Vries et al.* reads

$$u_{k,l} = \frac{\partial \chi}{\partial x} \Big|_{k,l} - \frac{\partial \psi}{\partial y} \Big|_{k,l} , \quad (B.9a)$$

$$v_{k,l} = \frac{\partial \chi}{\partial y} \Big|_{k,l} + \frac{\partial \psi}{\partial x} \Big|_{k,l} , \quad (B.9b)$$

with the subscripts k, l indicating that the quantity is to be evaluated at the grid point with indices k, l . On a discrete grid, the derivatives of a function f with respect to x and y reads [*Abramowitz and Stegun*, 1970, 25.3.21]

$$\frac{\partial f}{\partial x} \Big|_{k,l} = \frac{f_{k+1,l} - f_{k-1,l}}{2\Delta} , \quad \frac{\partial f}{\partial y} \Big|_{k,l} = \frac{f_{k,l+1} - f_{k,l-1}}{2\Delta} , \quad (B.10)$$

where Δ is the grid size which is assumed the same in both directions. Substitution of (B.10) in (B.9a) and replacing all quantities by their discrete inverse Fourier transforms yields

$$\begin{aligned} & \frac{1}{MN\Delta^2} \sum_{m=0}^{M-1} \sum_{n=0}^{N-1} \hat{u}_{m,n} e^{-2\pi i \left(\frac{km}{M} + \frac{ln}{N} \right)} = \\ & = \frac{1}{2\Delta} \left[\frac{1}{MN\Delta^2} \sum_{m=0}^{M-1} \sum_{n=0}^{N-1} \hat{\chi}_{m,n} e^{-2\pi i \left(\frac{(k+1)m}{M} + \frac{ln}{N} \right)} - \frac{1}{MN\Delta^2} \sum_{m=0}^{M-1} \sum_{n=0}^{N-1} \hat{\chi}_{m,n} e^{-2\pi i \left(\frac{(k-1)m}{M} + \frac{ln}{N} \right)} \right] + \\ & - \frac{1}{2\Delta} \left[\frac{1}{MN\Delta^2} \sum_{m=0}^{M-1} \sum_{n=0}^{N-1} \hat{\psi}_{m,n} e^{-2\pi i \left(\frac{km}{M} + \frac{(l+1)n}{N} \right)} - \frac{1}{MN\Delta^2} \sum_{m=0}^{M-1} \sum_{n=0}^{N-1} \hat{\psi}_{m,n} e^{-2\pi i \left(\frac{km}{M} + \frac{(l-1)n}{N} \right)} \right] . \end{aligned} \quad (B.11)$$

The normalization factors of the discrete inverse Fourier transform cancel. The exponentials at the right hand side of (B.11) can be expanded to yield

$$\begin{aligned} & \sum_{m=0}^{M-1} \sum_{n=0}^{N-1} \hat{u}_{m,n} e^{-2\pi i \left(\frac{km}{M} + \frac{ln}{N} \right)} = \\ & \frac{1}{2\Delta} \left[\sum_{m=0}^{M-1} \sum_{n=0}^{N-1} \hat{\chi}_{m,n} e^{-2\pi i \left(\frac{km}{M} + \frac{ln}{N} \right)} e^{2\pi i \frac{m}{M}} - \sum_{m=0}^{M-1} \sum_{n=0}^{N-1} \hat{\chi}_{m,n} e^{-2\pi i \left(\frac{km}{M} + \frac{ln}{N} \right)} e^{-2\pi i \frac{m}{M}} \right] + \\ & - \frac{1}{2\Delta} \left[\sum_{m=0}^{M-1} \sum_{n=0}^{N-1} \hat{\psi}_{m,n} e^{-2\pi i \left(\frac{km}{M} + \frac{ln}{N} \right)} e^{2\pi i \frac{n}{N}} - \sum_{m=0}^{M-1} \sum_{n=0}^{N-1} \hat{\psi}_{m,n} e^{-2\pi i \left(\frac{km}{M} + \frac{ln}{N} \right)} e^{-2\pi i \frac{n}{N}} \right] . \end{aligned} \quad (B.12)$$


This can be simplified to

$$\begin{aligned} & \sum_{m=0}^{M-1} \sum_{n=0}^{N-1} \hat{u}_{m,n} e^{-2\pi i \left(\frac{km}{M} + \frac{ln}{N} \right)} = \sum_{m=0}^{M-1} \sum_{n=0}^{N-1} e^{-2\pi i \left(\frac{km}{M} + \frac{ln}{N} \right)} \times \\ & \left[\hat{\chi}_{m,n} \left(\frac{e^{-2\pi i \frac{m}{M}} - e^{2\pi i \frac{m}{M}}}{2\Delta} \right) - \hat{\psi}_{m,n} \left(\frac{e^{-2\pi i \frac{n}{N}} - e^{2\pi i \frac{n}{N}}}{2\Delta} \right) \right] . \end{aligned} \quad (B.13)$$

This should hold for all m and n , so the summations and the common phase factor can be dropped. This results in

$$\hat{u}_{m,n} = \mu_m \hat{\chi}_{m,n} - \nu_n \hat{\psi}_{m,n} , \quad (B.14)$$

with

<div style="display: flex; align-items: center;"> <div style="margin-right: 10px;"> <small>The EUMETSAT Network of Satellite Application Facilities</small> </div> <div>  NWP SAF <small>Numerical Weather Prediction</small> </div> </div>	<h2 style="margin: 0;">Two-dimensional variational ambiguity removal (2DVAR)</h2>	Doc ID : NWPSAF-KN-TR-004 Version : 1.6 Date : 13-08-2021
--	---	---

$$\mu_m = \frac{1}{2\Delta} \left(e^{-2\pi i \frac{m}{M}} - e^{2\pi i \frac{m}{M}} \right) = \frac{-i}{2\Delta} \sin \left(2\pi \frac{m}{M} \right) , \quad (\text{B.15a})$$

$$\nu_n = \frac{1}{2\Delta} \left(e^{-2\pi i \frac{n}{N}} - e^{2\pi i \frac{n}{N}} \right) = \frac{-i}{2\Delta} \sin \left(2\pi \frac{n}{N} \right) . \quad (\text{B.15b})$$

In the same way, (B.9b) and (B.10) yield

$$\begin{aligned} \frac{1}{MN\Delta^2} \sum_{m=0}^{M-1} \sum_{n=0}^{N-1} \hat{v}_{m,n} e^{-2\pi i \left(\frac{km}{M} + \frac{ln}{N} \right)} = \\ \frac{1}{2\Delta} \left[\frac{1}{MN\Delta^2} \sum_{m=0}^{M-1} \sum_{n=0}^{N-1} \hat{\chi}_{m,n} e^{-2\pi i \left(\frac{km}{M} + \frac{(l+1)n}{N} \right)} - \frac{1}{MN\Delta^2} \sum_{m=0}^{M-1} \sum_{n=0}^{N-1} \hat{\chi}_{m,n} e^{-2\pi i \left(\frac{km}{M} + \frac{(l-1)n}{N} \right)} \right] + \\ + \frac{1}{2\Delta} \left[\frac{1}{MN\Delta^2} \sum_{m=0}^{M-1} \sum_{n=0}^{N-1} \hat{\psi}_{m,n} e^{-2\pi i \left(\frac{(k+1)m}{M} + \frac{ln}{N} \right)} - \frac{1}{MN\Delta^2} \sum_{m=0}^{M-1} \sum_{n=0}^{N-1} \hat{\psi}_{m,n} e^{-2\pi i \left(\frac{(k-1)m}{M} + \frac{ln}{N} \right)} \right] . \end{aligned} \quad (\text{B.16})$$

This can be written as

$$\begin{aligned} \sum_{m=0}^{M-1} \sum_{n=0}^{N-1} \hat{v}_{m,n} e^{-2\pi i \left(\frac{km}{M} + \frac{ln}{N} \right)} = \sum_{m=0}^{M-1} \sum_{n=0}^{N-1} e^{-2\pi i \left(\frac{km}{M} + \frac{ln}{N} \right)} \times \\ \frac{1}{2\Delta} \left[\hat{\chi}_{m,n} \left(e^{-2\pi i \frac{n}{N}} - e^{2\pi i \frac{n}{N}} \right) + \hat{\psi}_{m,n} \left(e^{-2\pi i \frac{m}{M}} - e^{2\pi i \frac{m}{M}} \right) \right] . \end{aligned} \quad (\text{B.17})$$

This simplifies to

$$\hat{v}_{m,n} = \nu_n \hat{\chi}_{m,n} + \mu_m \hat{\psi}_{m,n} , \quad (\text{B.18})$$

with μ and ν given by (B.15).

Comparison

Figure B.1 shows the Helmholtz transformation coefficients h_1 on the 2DVAR spatial frequency grid for the continuous boundary conditions (blue curve) and the periodic boundary conditions (red curve, with $h_1 = \mu$). The dots indicate the spatial frequency grid points. Figure B.1 shows that the two boundary conditions yield very similar transformation coefficients for low spatial frequencies ($p \approx 0$), but differences arise at higher frequencies. With periodic boundary conditions the transformation coefficients go to zero at high (positive and negative) frequencies, whereas the coefficients with continuous boundary conditions reach their extreme value there. The effect of the periodic boundary conditions is similar to that of applying a filter like the Hanning filter in an FFT operation: the spectrum is forced to zero at the ends of the interval. Since the background contribution to the cost function is calculated in the frequency domain, one may expect that the periodic boundary conditions yield smaller values than the continuous ones. This is indeed the case: in a single observation test the background contribution to the cost function at the solution is about 20% smaller when using periodic boundary conditions compared to the continuous boundary conditions.

Default 2DVAR uses the continuous boundary conditions. This is equivalent to taking a Fourier transform.

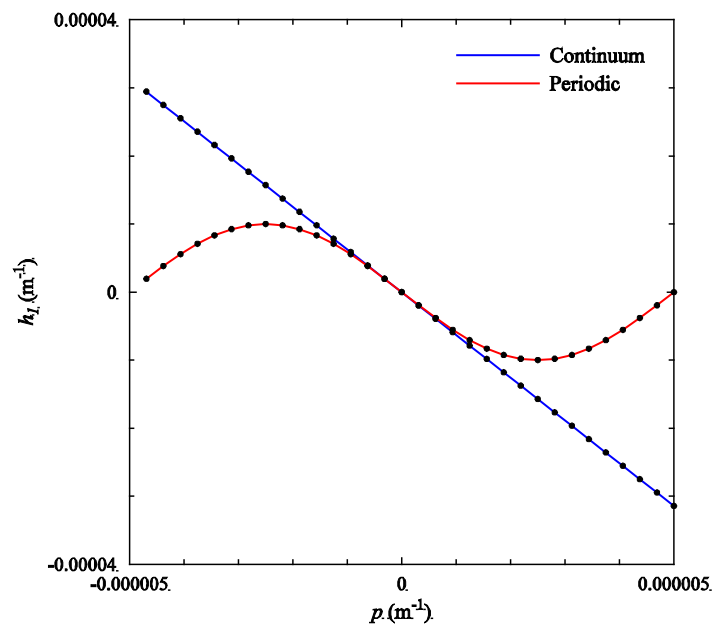



Figure B.1 Helmholtz transformation coefficients on the 2DVAR spatial frequency grid for the continuous boundary conditions (blue) and the discrete boundary conditions (red).

<p>The EUMETSAT Network of Satellite Application Facilities</p> 	<h1>Two-dimensional variational ambiguity removal (2DVAR)</h1>	<p>Doc ID : NWPSAF-KN-TR-004 Version : 1.6 Date : 13-08-2021</p>
---	--	--

Appendix C Helmholtz transformation in three dimensions

In three dimensions, any vector field $\mathbf{V} = (u, v, w)$ can be written as the sum of the gradient of a scalar potential χ and the rotation of a vector potential $\mathbf{\Psi} = (\Psi_x, \Psi_y, \Psi_z)$ as

$$\mathbf{V} = \nabla\chi + \nabla \times \mathbf{\Psi} \quad . \quad (\text{C.1})$$

Written out in Cartesian components, the terms in the right hand side of (A.1) read

$$\nabla\chi = \hat{\mathbf{e}}_x \frac{\partial\chi}{\partial x} + \hat{\mathbf{e}}_y \frac{\partial\chi}{\partial y} + \hat{\mathbf{e}}_z \frac{\partial\chi}{\partial z} \quad , \quad (\text{C.2a})$$

$$\nabla \times \mathbf{\Psi} = \hat{\mathbf{e}}_x \left[\frac{\partial\Psi_y}{\partial z} - \frac{\partial\Psi_z}{\partial y} \right] + \hat{\mathbf{e}}_y \left[\frac{\partial\Psi_z}{\partial x} - \frac{\partial\Psi_x}{\partial z} \right] + \hat{\mathbf{e}}_z \left[\frac{\partial\Psi_x}{\partial y} - \frac{\partial\Psi_y}{\partial x} \right] \quad , \quad (\text{C.2b})$$

with $\hat{\mathbf{e}}_x, \hat{\mathbf{e}}_y$, and $\hat{\mathbf{e}}_z$ the unit vectors in the x -, y -, and z -direction, respectively.

In two dimensions, all z -components vanish. Moreover, the potentials no longer depend on z , so all derivatives to z vanish. As a result


$$\nabla\chi|_2 = \hat{\mathbf{e}}_x \frac{\partial\chi}{\partial x} + \hat{\mathbf{e}}_y \frac{\partial\chi}{\partial y} \quad , \quad (\text{C.3a})$$


$$\nabla \times \mathbf{\Psi}|_2 = \hat{\mathbf{e}}_x \left[-\frac{\partial\Psi_z}{\partial y} \right] + \hat{\mathbf{e}}_y \left[\frac{\partial\Psi_z}{\partial x} \right] \quad , \quad (\text{C.3b})$$

with the subscript 2 indicating the transition to two dimensions. Note that only Ψ_z contributes to the vector field. Renaming it to ψ , dropping the subscript, and replacing the general vector field \mathbf{V} by the two dimensional wind field (u, v) , one obtains from (C.1) and (C.3)

$$u = \frac{\partial\chi}{\partial x} - \frac{\partial\psi}{\partial y} \quad , \quad v = \frac{\partial\chi}{\partial y} + \frac{\partial\psi}{\partial x} \quad . \quad (\text{C.4})$$

For a wind field, χ is referred to as the velocity potential and ψ as the stream function.

<p>The EUMETSAT Network of Satellite Application Facilities</p> 	<h1>Two-dimensional variational ambiguity removal (2DVAR)</h1>	<p>Doc ID : NWPSAF-KN-TR-004 Version : 1.6 Date : 13-08-2021</p>
---	--	--

 	Two-dimensional variational ambiguity removal (2DVAR)	Doc ID : NWPSAF-KN-TR-004 Version : 1.6 Date : 13-08-2021
---	---	---

Appendix D Adjoint model

Suppose we have a cost function J defined in the spatial domain as a function of a positional increment control vector \mathbf{x} as $J = J(\mathbf{x})$. Similarly, it can be defined in the frequency domain as a function of a spectral increment control vector $\boldsymbol{\xi}$ as $J = J(\boldsymbol{\xi})$. The two representations are connected by the unconditioning transformation \mathbf{U} according to $\mathbf{x} = \mathbf{U}\boldsymbol{\xi}$. Note that in the main text the positional increment control vector is denoted as $\delta\mathbf{x}$.

The sensitivity of the cost function to changes in \mathbf{x} can be studied by expanding it in a Taylor series around a point \mathbf{x}_0 and omitting terms of the second and higher order [Errico, 1997; Giering and Kaminski, 1998]

$$J(\mathbf{x}) = J(\mathbf{x}_0) + dJ \quad , \quad (\text{D.1})$$

with

$$dJ = \nabla_{\mathbf{x}} J \cdot (\mathbf{x} - \mathbf{x}_0) = \nabla_{\mathbf{x}} J \cdot d\mathbf{x} \quad . \quad (\text{D.2})$$

This is a scalar product, so (D.2) can be written as

$$dJ = \langle \nabla_{\mathbf{x}} J, d\mathbf{x} \rangle = \langle \nabla_{\mathbf{x}} J, \mathbf{U} d\boldsymbol{\xi} \rangle \quad , \quad (\text{D.3})$$

assuming that $d\mathbf{x} = \mathbf{U} d\boldsymbol{\xi}$.

Now the adjoint of \mathbf{U} is defined as the operator \mathbf{U}^* that satisfies

$$\langle \mathbf{x}_1, \mathbf{U}\mathbf{x}_2 \rangle = \langle \mathbf{U}^* \mathbf{x}_1, \mathbf{x}_2 \rangle \quad , \quad (\text{D.4})$$

for all \mathbf{x}_1 and \mathbf{x}_2 . In a finite dimensional space, which is the case for the control space (i.e., the space in which the control vectors are defined), the adjoint equals the complex conjugate of the transpose,

$$\mathbf{U}^* = \overline{\mathbf{U}^T} \quad . \quad (\text{D.5})$$

Applying this to (D.4) yields

$$dJ = \langle \mathbf{U}^* \nabla_{\mathbf{x}} J, d\boldsymbol{\xi} \rangle \quad . \quad (\text{D.6})$$

This can be recognized as the scalar product in the frequency domain. with $\mathbf{U}^* \nabla_{\mathbf{x}} J$ the gradient of J in the frequency domain. Therefore

$$\nabla_{\boldsymbol{\xi}} J = \mathbf{U}^* \nabla_{\mathbf{x}} J \quad . \quad (\text{D.7})$$


This gives the relation between the gradients of the cost function in both representations. The gradient of the observation term in the 2DVAR cost function is evaluated in the spatial domain, and can be transformed to the frequency domain using (D.7). Note that the cost function is invariant under change of domain.

In chapter 3, equation (3.17) it was shown that the unconditioning transformation reads

$$\mathbf{U} = \mathbf{F}^{-1} \mathbf{H} \mathbf{B}_{\hat{\lambda}, \hat{\psi}}^{1/2} \quad . \quad (\text{D.8})$$

From the definition of the adjoint it follows that

$$\mathbf{U}^* = \left(\mathbf{F}^{-1} \mathbf{H} \mathbf{B}_{\hat{\lambda}, \hat{\psi}}^{1/2} \right)^* = \left(\mathbf{B}_{\hat{\lambda}, \hat{\psi}}^{1/2} \right)^* \mathbf{H}^* (\mathbf{F}^{-1})^* \quad . \quad (\text{D.9})$$

<div style="display: flex; align-items: center;"> <div style="margin-right: 20px;"> <small>The EUMETSAT Network of Satellite Application Facilities</small> </div> <div>  NWP SAF <small>Numerical Weather Prediction</small> </div> </div>	<h2>Two-dimensional variational ambiguity removal (2DVAR)</h2>	Doc ID : NWPSAF-KN-TR-004 Version : 1.6 Date : 13-08-2021
--	--	---

The inverse Fourier transform is defined in appendix A. It is easily shown that $(F^{-1})^* = F$. The Helmholtz transformation involves multiplication of the spectra components with an imaginary factor, which changes sign in the adjoint case. The normalization involves multiplication with a real factor. With this, (D.9) can be written as

$$\mathbf{U}^* = \mathbf{B}_{\hat{\chi}, \hat{\psi}}^{1/2} \mathbf{H}^* F^{-1} \quad . \quad (\text{D.10})$$

Adjoint of the Helmholtz transformation

The adjoint of the Helmholtz transformation in Fourier space, H^* , can be found from (3.6) by writing it as

$$\begin{pmatrix} \hat{t} \\ \hat{l} \end{pmatrix} = \mathbf{H} \begin{pmatrix} \hat{\chi} \\ \hat{\psi} \end{pmatrix} = -2\pi i \begin{pmatrix} p & -q \\ q & p \end{pmatrix} \begin{pmatrix} \hat{\chi} \\ \hat{\psi} \end{pmatrix} \quad , \quad (\text{D.11})$$

omitting the arguments of the velocities and the potentials. From (D.11) it easily follows that

$$\mathbf{H}^* = 2\pi i \begin{pmatrix} p & q \\ -q & p \end{pmatrix} \quad . \quad (\text{D.12})$$

The adjoint transformation reads

$$\begin{pmatrix} d\hat{\chi} \\ d\hat{\psi} \end{pmatrix} = \mathbf{H}^* \begin{pmatrix} d\hat{t} \\ d\hat{l} \end{pmatrix} \quad , \quad (\text{D.13})$$

or expanded in components

$$d\hat{\chi} = 2\pi i p d\hat{t} + 2\pi i q d\hat{l} \quad , \quad (\text{D.14a})$$

$$d\hat{\psi} = -2\pi i q d\hat{t} + 2\pi i p d\hat{l} \quad . \quad (\text{D.14b})$$

Appendix E Single Observation Analysis

Basic principles

Suppose the observation increment is denoted by o , the background increment by b , and the analysis increment by a . The cost function can be written as

$$J_t = J_o + J_b = \frac{(o-a)^2}{\varepsilon_o^2} + \frac{(b-a)^2}{\varepsilon_b^2} \quad , \quad (E.1)$$

where ε_o stands for the standard deviation of the observation error and ε_b that of the background error. Equation (E.1) is at a higher level of abstraction than the remainder of this report, but that simplifies the derivation. The optimal analysis is obtained by minimizing the total cost function with respect to the analysis. At the optimal analysis increment the derivative of the total cost function should be zero,

$$\frac{\partial J_t}{\partial a} = \frac{2(o-a)}{\varepsilon_o^2} + \frac{2(b-a)}{\varepsilon_b^2} = 2 \frac{\varepsilon_b^2 o + \varepsilon_o^2 b - (\varepsilon_o^2 + \varepsilon_b^2) a}{\varepsilon_o^2 \varepsilon_b^2} = 0 \quad . \quad (E.2)$$

This is satisfied for

$$a = \frac{\varepsilon_b^2 o + \varepsilon_o^2 b}{\varepsilon_o^2 + \varepsilon_b^2} \quad . \quad (E.3)$$

The optimal analysis increment is just the weighted average of the observation and the background increments. For $\varepsilon_b = \varepsilon_o$ the single observation solution reduces to $a = \frac{1}{2}(o + b)$.

Starting with zero background and analysis increments, the only contribution to the initial cost function is from the observation part, so it reads

$$J_t^{ini} = J_o^{ini} = \frac{o^2}{\varepsilon_o^2} \quad . \quad (E.4)$$

At the optimal analysis increment it reads (substitute (E.3) into (E.1))

$$J_t^{fin} = \frac{(o-a)^2}{\varepsilon_o^2} + \frac{(b-a)^2}{\varepsilon_b^2} = \frac{(o-b)^2}{\varepsilon_o^2 + \varepsilon_b^2} \quad . \quad (E.5)$$

The initial gradient reads



$$\nabla J_t^{ini} = \nabla J_o^{ini} = \frac{2o}{\varepsilon_o^2} \quad . \quad (E.6)$$

The total gradient at the optimal analysis, $\nabla J_t^{fin} = \nabla J_o^{fin} + \nabla J_b^{fin}$ equals zero, so $\nabla J_o^{fin} = -\nabla J_b^{fin}$, and therefore

$$\nabla J_o^{fin} = \frac{\partial J_t^{fin}}{\partial o} = \frac{\partial}{\partial o} \left[\frac{(o-b)^2}{\varepsilon_o^2 + \varepsilon_b^2} \right] = \frac{2(o-b)}{\varepsilon_o^2 + \varepsilon_b^2} = -\nabla J_b^{fin} \quad . \quad (E.7)$$

Since in the incremental approach $o - b = o$, (E.6) and (E.7) can be combined into

$$\nabla J_b^{fin} = \frac{-2o}{\varepsilon_o^2 + \varepsilon_b^2} = \frac{-\varepsilon_o^2}{\varepsilon_o^2 + \varepsilon_b^2} \nabla J_t^{ini} = \frac{-\varepsilon_o^2}{\varepsilon_o^2 + \varepsilon_b^2} \nabla J_o^{ini} \quad , \quad (E.8)$$

 	Two-dimensional variational ambiguity removal (2DVAR)	Doc ID : NWPSAF-KN-TR-004 Version : 1.6 Date : 13-08-2021
---	--	---

where has been used that (E.6) is equivalent to $o = \frac{1}{2} \varepsilon_o^2 \nabla J_o^{ini}$. Equation (E.8) relates the gradient in the final background cost to that of the initial observation cost. According to (3.18) - (3.20), the gradient in the final background cost is directly related to the analysis wind components $\hat{\psi}^{(n)}(p, q)$ and $\hat{\chi}^{(n)}(p, q)$, because in terms of the control vector ξ one has $J_B = \xi \cdot \xi$, so $\nabla J_B = 2\xi$. This holds during the whole minimisation procedure, so it also holds for the final cost function gradient, $\nabla J_B^{fin} = 2\xi^{fin}$. With the help of (E.8), the final control vector ξ^{fin} , i.e., the final values of $\hat{\psi}^{(n)}(p, q)$ and $\hat{\chi}^{(n)}(p, q)$, can be related to the initial observation cost function.

An analytic expression of the single observation analysis can be obtained from the following steps:

- Start with the gradient of the initial observation cost function;
- Transform this to the normalized stream function and velocity potential in the spatial frequency domain using the adjoint of the unconditioning transformation $\mathbf{U}^* = \mathbf{B}_{\chi, \hat{\psi}}^{1/2} \mathbf{H}^* \mathbf{F}^{-1}$ as given by (4.5) and (D.10);
- Apply relation (E.8) to write this in terms of the final analysis stream function and velocity potential;
- Transform this to the analysis wind field with the unconditioning transformation (3.17), $\mathbf{U} = \mathbf{F}^{-1} \mathbf{H} \mathbf{B}_{\chi, \hat{\psi}}^{1/2}$.

Analytic expression for Gaussian structure functions

Suppose a single wind vector observation (t_o, l_o) is available at the point $(x, y) = (0, 0)$. The components of the gradient of the observational part of the cost function, denoted as dt_o and dl_o , can be obtained from (4.10) (or (E.6)) as

$$dt_o(x, y) = \frac{\partial J_o^{ini}}{\partial \delta t} = -\frac{2t_o}{\varepsilon_o^2} \delta(x, y) \quad , \quad dl_o(x, y) = \frac{\partial J_o^{ini}}{\partial \delta l} = -\frac{2l_o}{\varepsilon_o^2} \delta(x, y) \quad , \quad (\text{E.9})$$

with $\delta(x, y)$ the Dirac delta function in two dimensional position and $\varepsilon_o = \varepsilon_t = \varepsilon_l$ the standard deviation of the error in the observed wind speed components. The gradient has to be taken with respect to the observation increments δt and δl . The delta function appears because the gradient is zero everywhere except at $(0, 0)$ where the observation is located. In this representation, the observation wind field is considered as a function in two dimensional position space rather than a discrete function on a two dimensional grid. The notation dt_o and dl_o is introduced to simplify the notation and to keep in line with the 2DVAR code in genscat.



Adjoint unconditioning transformation

The components of the observation cost function gradient in spatial frequency space, $d\hat{u}_o$ and $d\hat{v}_o$, are found by applying the adjoint of the inverse Fourier transformation. This just equals the forward Fourier transformation (A.1). Due to the delta function, the integrals are easily evaluated, yielding

$$d\hat{u}_o(p, q) = - \iint dxdy \frac{2t_o}{\varepsilon_o^2} \delta(x, y) e^{2\pi i(px+qy)} = -\frac{2t_o}{\varepsilon_o^2} \quad , \quad (\text{E.10a})$$

$$d\hat{v}_o(p, q) = - \iint dxdy \frac{2l_o}{\varepsilon_o^2} \delta(x, y) e^{2\pi i(px+qy)} = -\frac{2l_o}{\varepsilon_o^2} \quad . \quad (\text{E.10b})$$

Note that the cost function gradient in the spatial frequency domain is constant.

 	Two-dimensional variational ambiguity removal (2DVAR)	Doc ID : NWPSAF-KN-TR-004 Version : 1.6 Date : 13-08-2021
---	--	---

The next step is to apply the adjoint of the forward Helmholtz transformation (3.6) to get the gradient components of the stream function and the velocity potential $d\hat{\psi}_O$ and $d\hat{\chi}_O$ as

$$d\hat{\psi}_O(p, q) = 2\pi i[-qd\hat{u}_O(p, q) + pd\hat{v}_O(p, q)] = -\frac{4\pi i}{\varepsilon_O^2}(l_0p - t_0q) \quad , \quad (\text{E.11a})$$

$$d\hat{\chi}_O(p, q) = 2\pi i[pd\hat{u}_O(p, q) + qd\hat{v}_O(p, q)] = -\frac{4\pi i}{\varepsilon_O^2}(t_0p + l_0q) \quad . \quad (\text{E.11b})$$

To arrive at the gradient components of the normalized stream function and the normalized velocity potential, one must multiply with the adjoint of the background error covariance matrix in the spatial frequency domain, $B_{\hat{\psi}\hat{\psi}}^{1/2}$ and $B_{\hat{\chi}\hat{\chi}}^{1/2}$. These are real quantities given by (6.7). Setting $R = R_\psi = R_\chi$ and $\varepsilon_B = \varepsilon_l = \varepsilon_t$ one readily finds

$$d\hat{\psi}_O^{(n)}(p, q) = -4\pi i \sqrt{\frac{\pi}{2}(1 - \nu^2)} \frac{\varepsilon_B}{\varepsilon_O^2} R^2(l_0p - t_0q) e^{-\frac{1}{2}\pi^2 R^2(p^2 + q^2)} \quad , \quad (\text{E.12a})$$

$$d\hat{\chi}_O^{(n)}(p, q) = -4\pi i \sqrt{\frac{\pi}{2}\nu^2} \frac{\varepsilon_B}{\varepsilon_O^2} R^2(t_0p + l_0q) e^{-\frac{1}{2}\pi^2 R^2(p^2 + q^2)} \quad . \quad (\text{E.12b})$$

From observation gradient to analysis

Now the results of chapter 7 can be applied to calculate the analysis. According to (E.8) and the discussion following it

$$\xi = \frac{1}{2} \nabla J_B^{fin} = -\frac{1}{2} \varepsilon_O^2 (\varepsilon_O^2 + \varepsilon_B^2)^{-1} \nabla J_O^{ini} \quad , \quad (\text{E.13})$$

which translates into

$$\hat{\psi}^{(n)}(p, q) = -\frac{1}{2} \frac{\varepsilon_O^2}{\varepsilon_O^2 + \varepsilon_B^2} d\hat{\psi}_O^{(n)}(p, q) \quad , \quad (\text{E.14a})$$

$$\hat{\chi}^{(n)}(p, q) = -\frac{1}{2} \frac{\varepsilon_O^2}{\varepsilon_O^2 + \varepsilon_B^2} d\hat{\chi}_O^{(n)}(p, q) \quad . \quad (\text{E.14b})$$

From (E.14) and (E.12) one readily finds

$$\hat{\psi}^{(n)}(p, q) = 2\pi i \sqrt{\frac{\pi}{2}(1 - \nu^2)} \frac{\varepsilon_B}{\varepsilon_O^2 + \varepsilon_B^2} R^2(l_0p - t_0q) e^{-\frac{1}{2}\pi^2 R^2(p^2 + q^2)} \quad , \quad (\text{E.15a})$$

$$\hat{\chi}^{(n)}(p, q) = 2\pi i \sqrt{\frac{\pi}{2}\nu^2} \frac{\varepsilon_B}{\varepsilon_O^2 + \varepsilon_B^2} R^2(t_0p + l_0q) e^{-\frac{1}{2}\pi^2 R^2(p^2 + q^2)} \quad . \quad (\text{E.15b})$$



Now it is possible to transform (E.15a-b) back to the spatial domain.

Unconditioning transformation

Multiplying (E.15) with the background error covariance matrix in the spatial frequency domain, $B_{\hat{\psi}\hat{\psi}}^{1/2}$ and $B_{\hat{\chi}\hat{\chi}}^{1/2} \Lambda_\psi^{1/2} \Lambda_\chi^{1/2}$, yields

$$\hat{\psi}(p, q) = i\pi^2 \frac{\varepsilon_B^2}{\varepsilon_O^2 + \varepsilon_B^2} R^4(1 - \nu^2)(l_0p - t_0q) e^{-\pi^2 R^2(p^2 + q^2)} \quad , \quad (\text{E.16a})$$

$$\hat{\chi}(p, q) = i\pi^2 \frac{\varepsilon_B^2}{\varepsilon_O^2 + \varepsilon_B^2} R^4\nu^2(t_0p + l_0q) e^{-\pi^2 R^2(p^2 + q^2)} \quad , \quad (\text{E.16b})$$

 	Two-dimensional variational ambiguity removal (2DVAR)	Doc ID : NWPSAF-KN-TR-004 Version : 1.6 Date : 13-08-2021
---	--	---

again setting $R = R_\psi = R_\chi$ and $\varepsilon_B = \varepsilon_l = \varepsilon_t$.

Application of the forward Helmholtz transformation (3.6) results in

$$\hat{t}(p, q) = 2\pi^3 \frac{\varepsilon_B^2}{\varepsilon_O^2 + \varepsilon_B^2} R^4 [pv^2(t_0p + l_0q) - q(1 - v^2)(l_0p - t_0q)] e^{-\pi^2 R^2(p^2 + q^2)} \quad , \quad (\text{E.17a})$$

$$\hat{l}(p, q) = 2\pi^3 \frac{\varepsilon_B^2}{\varepsilon_O^2 + \varepsilon_B^2} R^4 [qv^2(t_0p + l_0q) + p(1 - v^2)(l_0p - t_0q)] e^{-\pi^2 R^2(p^2 + q^2)} \quad . \quad (\text{E.17b})$$

This can be written as

$$\hat{t}(p, q) = 2\pi^3 \frac{\varepsilon_B^2}{\varepsilon_O^2 + \varepsilon_B^2} R^4 [v^2 t_0 p^2 + (2v^2 - 1)l_0 p q + (1 - v^2)t_0 q^2] e^{-\pi^2 R^2(p^2 + q^2)} \quad , \quad (\text{E.18a})$$

$$\hat{l}(p, q) = 2\pi^3 \frac{\varepsilon_B^2}{\varepsilon_O^2 + \varepsilon_B^2} R^4 [(1 - v^2)l_0 p^2 + (2v^2 - 1)t_0 p q + v^2 l_0 q^2] e^{-\pi^2 R^2(p^2 + q^2)} \quad . \quad (\text{E.18b})$$

Inverse Fourier transformation (A.2) finally yields

$$t(x, y) = \frac{2\pi^3 \varepsilon_B^2 R^4}{\varepsilon_O^2 + \varepsilon_B^2} [v^2 t_0 I_{pp}(x, y; a) + (2v^2 - 1)l_0 I_{pq}(x, y; a) + (1 - v^2)t_0 I_{qq}(x, y; a)] \quad , \quad (\text{E.19a})$$

$$l(x, y) = \frac{2\pi^3 \varepsilon_B^2 R^4}{\varepsilon_O^2 + \varepsilon_B^2} [(1 - v^2)l_0 I_{pp}(x, y; a) + (2v^2 - 1)t_0 I_{pq}(x, y; a) + v^2 l_0 I_{qq}(x, y; a)] \quad , \quad (\text{E.19b})$$

where $a = \pi^2 R^2$ and the integrals are defined as

$$I_{pp}(x, y; a) = \int_{-\infty}^{\infty} dp \int_{-\infty}^{\infty} dq \quad p^2 e^{-a(p^2 + q^2)} e^{-2\pi i(px + qy)} \quad , \quad (\text{E.20a})$$

$$I_{pq}(x, y; a) = \int_{-\infty}^{\infty} dp \int_{-\infty}^{\infty} dq \quad pq^2 e^{-a(p^2 + q^2)} e^{-2\pi i(px + qy)} \quad , \quad (\text{E.20b})$$

$$I_{qq}(x, y; a) = \int_{-\infty}^{\infty} dp \int_{-\infty}^{\infty} dq \quad q^2 e^{-a(p^2 + q^2)} e^{-2\pi i(px + qy)} \quad , \quad (\text{E.20c})$$

These integrals are calculated in Appendix G. With $a = \pi^2 R^2$ one obtains from (G.16)

$$I_{pp}(x, y; a) = \frac{1}{\pi^3 R^4} \left[-\frac{x^2}{R^2} + \frac{1}{2} \right] e^{-\frac{x^2 + y^2}{R^2}} \quad , \quad (\text{E.21a})$$

$$I_{pq}(x, y; a) = \frac{-1}{\pi^3 R^4} \frac{xy}{R^2} e^{-\frac{x^2 + y^2}{R^2}} \quad , \quad (\text{E.21b})$$



$$I_{qq}(x, y; a) = \frac{1}{\pi^3 R^4} \left[-\frac{y^2}{R^2} + \frac{1}{2} \right] e^{-\frac{x^2 + y^2}{R^2}} \quad . \quad (\text{E.21c})$$

This immediately yields the final result for the single observation analysis

$$t(x, y) = \frac{\varepsilon_B^2}{\varepsilon_O^2 + \varepsilon_B^2} \left[v^2 t_0 \left(1 - \frac{2x^2}{R^2} \right) - (4v^2 - 2)l_0 \frac{xy}{R^2} + (1 - v^2)t_0 \left(1 - \frac{2y^2}{R^2} \right) \right] e^{-\frac{x^2 + y^2}{R^2}} \quad , \quad (\text{E.22a})$$

$$l(x, y) = \frac{\varepsilon_B^2}{\varepsilon_O^2 + \varepsilon_B^2} \left[(1 - v^2)l_0 \left(1 - \frac{2x^2}{R^2} \right) - (4v^2 - 2)t_0 \frac{xy}{R^2} + v^2 l_0 \left(1 - \frac{2y^2}{R^2} \right) \right] e^{-\frac{x^2 + y^2}{R^2}} \quad . \quad (\text{E.22b})$$

Remember that we started with the observation (t_0, l_0) at the origin. However, if the observation is at some other location, the analytical expression for the single observation analysis is easily obtained from (E.22) by a shift in coordinates.

 	Two-dimensional variational ambiguity removal (2DVAR)	Doc ID : NWPSAF-KN-TR-004 Version : 1.6 Date : 13-08-2021
---	--	---

Special values

For $x = y = 0$ equation (E.22) reduces to

$$t(0,0) = \frac{\varepsilon_B^2}{\varepsilon_B^2 + \varepsilon_O^2} t_0 \quad , \quad l(0,0) = \frac{\varepsilon_B^2}{\varepsilon_B^2 + \varepsilon_O^2} l_0 \quad . \quad (\text{E.23})$$

This is the weighted average of observation and the background. If $\varepsilon_B \rightarrow 0$, i.e., if the background is free of errors, the analysis increment vanishes. Since the analysis is defined as the “true” wind field minus the background, this implies that the true wind field equals the background – which should be the case if the background is free of errors.

If, on the other hand, $\varepsilon_B \rightarrow \infty$, i.e., if the background is completely unreliable and contains no information, the analysis increment gets its maximum value and is determined by the observation – the only information source at hand.

If $\varepsilon_B = \varepsilon_O$, equation (E.23) yields $t(0,0) = \frac{1}{2} t_0$ and $l(0,0) = \frac{1}{2} l_0$.

General single observation analysis

In the general case, i.e., for non-Gaussian background error covariances, one can start from (E.11a-b) and multiply with the adjoint of the background error covariance matrix in the spatial frequency domain, $B_{\hat{\psi}\hat{\psi}}^{1/2}$ and $B_{\hat{\chi}\hat{\chi}}^{1/2}$ to obtain

$$d\hat{\psi}_O^{(n)}(p, q) = -\frac{4\pi i}{\varepsilon_O^2} (l_0 p - t_0 q) B_{\hat{\psi}\hat{\psi}}^{1/2} \quad , \quad (\text{E.24a})$$

$$d\hat{\chi}_O^{(n)}(p, q) = -\frac{4\pi i}{\varepsilon_O^2} (t_0 p + l_0 q) B_{\hat{\chi}\hat{\chi}}^{1/2} \quad , \quad (\text{E.24b})$$

where again the fact has been used that the background error covariances are real, thus self-adjoint. Applying (E.14) to write (E.24) in terms of the analysis yields

$$\hat{\psi}^{(n)}(p, q) = \frac{2\pi i}{\varepsilon_O^2 + \varepsilon_B^2} (l_0 p - t_0 q) B_{\hat{\psi}\hat{\psi}}^{1/2} \quad , \quad (\text{E.25a})$$

$$\hat{\chi}^{(n)}(p, q) = \frac{2\pi i}{\varepsilon_O^2 + \varepsilon_B^2} (t_0 p + l_0 q) B_{\hat{\chi}\hat{\chi}}^{1/2} \quad . \quad (\text{E.25b})$$

Multiplying (E.25) with the background error covariance matrix in the spatial frequency domain, $B_{\hat{\psi}\hat{\psi}}^{1/2}$ and $B_{\hat{\chi}\hat{\chi}}^{1/2}$, and writing $\hat{f}_\psi = B_{\hat{\psi}\hat{\psi}} \hat{\psi}$, $\hat{f}_\chi = B_{\hat{\chi}\hat{\chi}} \hat{\chi}$ yields

$$\hat{\psi}(p, q) = \frac{2\pi i}{\varepsilon_O^2 + \varepsilon_B^2} (l_0 p - t_0 q) \hat{f}_\psi(p, q) \quad , \quad (\text{E.26a})$$

$$\hat{\chi}(p, q) = \frac{2\pi i}{\varepsilon_O^2 + \varepsilon_B^2} (t_0 p + l_0 q) \hat{f}_\chi(p, q) \quad . \quad (\text{E.26b})$$

Applying the forward Helmholtz transformation (3.6) gives

$$\hat{t}(p, q) = \frac{4\pi^2}{\varepsilon_O^2 + \varepsilon_B^2} [(t_0 p^2 + l_0 p q) \hat{f}_\chi(p, q) - (l_0 p q - t_0 q^2) \hat{f}_\psi(p, q)] \quad , \quad (\text{E.27a})$$

$$\hat{l}(p, q) = \frac{4\pi^2}{\varepsilon_O^2 + \varepsilon_B^2} [(t_0 p q + l_0 q^2) \hat{f}_\chi(p, q) + (l_0 p^2 - t_0 p q) \hat{f}_\psi(p, q)] \quad . \quad (\text{E.27b})$$

The analysis wind fields are obtained by applying the inverse Fourier transformation (A.2) to (E.27)

$$t(x, y) = \frac{4\pi^2}{\varepsilon_0^2 + \varepsilon_B^2} dpdq e^{-2\pi i(px+qy)} [(t_0 p^2 + l_0 pq) \hat{f}_\chi(p, q) - (l_0 pq - t_0 q^2) \hat{f}_\psi(p, q)] \quad , \quad (\text{E.28a})$$

$$l(x, y) = \frac{4\pi^2}{\varepsilon_0^2 + \varepsilon_B^2} dpdq e^{-2\pi i(px+qy)} [(t_0 pq + l_0 q^2) \hat{f}_\chi(p, q) + (l_0 p^2 - t_0 pq) \hat{f}_\psi(p, q)] \quad . \quad (\text{E.28b})$$

The integrals in (E.28) can be evaluated by noting that

$$\frac{df(x)}{dx} = \frac{d}{dx} \int dp e^{-2\pi i p x} \hat{f}(p) = -2\pi i \int dp e^{-2\pi i p x} p \hat{f}(p) \quad , \quad (\text{E.29})$$

from which it follows that

$$\int dp e^{-2\pi i p x} p \hat{f}(p) = \frac{i}{2\pi} \frac{df(x)}{dx} \quad . \quad (\text{E.30})$$

Applying (E.30) to (E.28) finally yields

$$t(x, y) = \frac{-1}{\varepsilon_0^2 + \varepsilon_B^2} \left[t_0 \left(\frac{\partial^2 f_\chi(x, y)}{\partial x^2} + \frac{\partial^2 f_\psi(x, y)}{\partial y^2} \right) + l_0 \left(\frac{\partial^2 f_\chi(x, y)}{\partial x \partial y} - \frac{\partial^2 f_\psi(x, y)}{\partial x \partial y} \right) \right] \quad , \quad (\text{E.31a})$$

$$l(x, y) = \frac{-1}{\varepsilon_0^2 + \varepsilon_B^2} \left[l_0 \left(\frac{\partial^2 f_\chi(x, y)}{\partial y^2} + \frac{\partial^2 f_\psi(x, y)}{\partial x^2} \right) + t_0 \left(\frac{\partial^2 f_\chi(x, y)}{\partial x \partial y} - \frac{\partial^2 f_\psi(x, y)}{\partial x \partial y} \right) \right] \quad . \quad (\text{E.31b})$$

Equation (E.31) shows that the single observation analysis is determined by the double derivatives of the background error covariances (which are defined in the spatial potential domain), rather than their values. For Gaussian error covariances the spatial extent of the single observation analysis is of the same order of magnitude as that of the background error correlations, but in general this needs not be the case.

Finally, substituting (6.1) into (E.31) yields (E.22). Starting from (6.1a-b) with $R_\psi = R_\chi = R$, $V_l = V_t = \varepsilon_B^2$, and $L_\psi^2 = L_\chi^2 = \frac{1}{2} R^2$ one finds

$$f_\psi(r) = \frac{1}{2} (1 - \nu^2) \varepsilon_B^2 R^2 e^{-\frac{r^2}{R^2}} \quad , \quad f_\chi(r) = \frac{1}{2} \nu^2 \varepsilon_B^2 R^2 e^{-\frac{r^2}{R^2}} \quad , \quad (\text{E.32})$$

with derivatives


$$\frac{\partial^2 f_\psi(r)}{\partial x^2} = (1 - \nu^2) \varepsilon_B^2 \left(\frac{2x^2}{R^2} - 1 \right) e^{-\frac{r^2}{R^2}} \quad , \quad \frac{\partial^2 f_\chi(r)}{\partial x^2} = \nu^2 \varepsilon_B^2 \left(\frac{2x^2}{R^2} - 1 \right) e^{-\frac{r^2}{R^2}} \quad , \quad (\text{E.33a})$$

$$\frac{\partial^2 f_\psi(r)}{\partial x \partial y} = (1 - \nu^2) \varepsilon_B^2 \frac{2xy}{R^2} e^{-\frac{r^2}{R^2}} \quad , \quad \frac{\partial^2 f_\chi(r)}{\partial x \partial y} = \nu^2 \varepsilon_B^2 \frac{2xy}{R^2} e^{-\frac{r^2}{R^2}} \quad , \quad (\text{E.33b})$$


$$\frac{\partial^2 f_\psi(r)}{\partial y^2} = (1 - \nu^2) \varepsilon_B^2 \left(\frac{2y^2}{R^2} - 1 \right) e^{-\frac{r^2}{R^2}} \quad , \quad \frac{\partial^2 f_\chi(r)}{\partial y^2} = \nu^2 \varepsilon_B^2 \left(\frac{2y^2}{R^2} - 1 \right) e^{-\frac{r^2}{R^2}} \quad . \quad (\text{E.33c})$$

Substitution of (E.33) in (E.31a) yields

$$\begin{aligned} t(x, y) &= \frac{-\varepsilon_B^2}{\varepsilon_0^2 + \varepsilon_B^2} \left[t_0 \left(\nu^2 \left(\frac{2x^2}{R^2} - 1 \right) + (1 - \nu^2) \left(\frac{2y^2}{R^2} - 1 \right) \right) + l_0 \left(\nu^2 \frac{2xy}{R^2} - (1 - \nu^2) \frac{2xy}{R^2} \right) \right] e^{-\frac{r^2}{R^2}} = \\ &= \frac{\varepsilon_B^2}{\varepsilon_0^2 + \varepsilon_B^2} \left[\nu^2 t_0 \left(1 - \frac{2x^2}{R^2} \right) - (4\nu^2 - 2) l_0 \frac{xy}{R^2} + (1 - \nu^2) t_0 \left(1 - \frac{2y^2}{R^2} \right) \right] e^{-\frac{r^2}{R^2}} \quad , \end{aligned}$$

<div data-bbox="140 129 256 185"> The EUMETSAT Network of Satellite Application Facilities </div> <div data-bbox="284 141 550 215">  NWP SAF Numerical Weather Prediction </div>	<h1>Two-dimensional variational ambiguity removal (2DVAR)</h1>	Doc ID : NWPSAF-KN-TR-004 Version : 1.6 Date : 13-08-2021
--	--	---

which is identical to (E.22a). The equivalence between (E.31b) and (E.22b) can be shown in the same manner.

<p>The EUMETSAT Network of Satellite Application Facilities</p> 	<h1>Two-dimensional variational ambiguity removal (2DVAR)</h1>	<p>Doc ID : NWPSAF-KN-TR-004 Version : 1.6 Date : 13-08-2021</p>
---	--	--

Appendix F Single observation analysis for EBECs

Empirical background error correlations

It has been shown by *Vogelzang and Stoffelen* [2011] that empirical background error correlations (EBECs) can be derived from O-B covariances under reasonable assumptions. Their results read

$$\rho_{\psi\psi}(r) = 1 + \frac{S(r)-R(r)}{2a_{\psi}} \quad , \quad \rho_{\chi\chi}(r) = 1 + \frac{S(r)+R(r)}{2a_{\chi}} \quad , \quad (\text{F.1})$$

with

$$R(r) = \int_0^r ds \, sI(s) \quad , \quad S(r) = \int_0^r ds \, \frac{J(s)}{s} \quad , \quad (\text{F.2})$$

and

$$I(r) = \int_r^\infty ds \, \frac{\rho_{tt}(s)-\rho_{ll}(s)}{s} \quad , \quad J(r) = \int_0^r ds \, s(\rho_{tt}(s) + \rho_{ll}(s)) \quad , \quad (\text{F.3})$$

where ρ_{tt} and ρ_{ll} are the O-B correlations for the cross-track and along-track wind components, t and l , respectively.

The parameters a_{ψ} and a_{χ} are determined by the requirement that the EBECs approach zero when r goes to infinity as

$$a_{\psi} = -\frac{1}{2}(S(\infty) - R(\infty)) \quad , \quad a_{\chi} = -\frac{1}{2}(S(\infty) + R(\infty)) \quad . \quad (\text{F.4})$$

The length scales L_{ψ} and L_{χ} are

$$L_{\psi}^2 = -\frac{2a_{\psi}}{1-I(0)} \quad , \quad L_{\chi}^2 = -\frac{2a_{\chi}}{1+I(0)} \quad . \quad (\text{F.5})$$

Since $a_{\psi} = -L_{\psi}^2(1 - \nu^2)$ and $a_{\chi} = -L_{\chi}^2\nu^2$ it follows from (F.5) that the divergence to rotation ratio ν^2 is given by

$$\nu^2 = \frac{1}{2}(1 + I(0)) \quad . \quad (\text{F.6})$$

Note that in the same notation as above the Gaussian background error correlations have the form


$$\rho_{\chi\chi}^{(G)}(r) = \exp\left(-\frac{r^2}{R_{\chi}^2}\right) \quad , \quad \rho_{\psi\psi}^{(G)}(r) = \exp\left(-\frac{r^2}{R_{\psi}^2}\right) \quad , \quad (\text{F.7})$$

which agrees with the definitions in chapter 6.

Derivatives to x and y

The EBECs (F.1) are functions of the distance r only. Now for any function $F(r)$

$$\frac{\partial F(r)}{\partial x} = \frac{dF(r)}{dr} \frac{dr}{dx} = F'(r) \frac{x}{r} = x \frac{F'(r)}{r} \quad , \quad (\text{F.8a})$$

<div style="display: flex; align-items: center;"> <div style="margin-right: 20px;"> <small>The EUMETSAT Network of Satellite Application Facilities</small> </div> <div>  NWP SAF <small>Numerical Weather Prediction</small> </div> </div>	<h2>Two-dimensional variational ambiguity removal (2DVAR)</h2>	Doc ID : NWPSAF-KN-TR-004 Version : 1.6 Date : 13-08-2021
--	--	---

$$\frac{\partial F(r)}{\partial y} = \frac{dF(r)}{dr} \frac{dr}{dy} = F'(r) \frac{y}{r} = y \frac{F'(r)}{r} , \quad (\text{F.8b})$$

where the prime denotes differentiation to r . From (F.8)

$$\frac{\partial^2 F(r)}{\partial x^2} = \frac{\partial}{\partial x} \left[x \frac{F'(r)}{r} \right] = \frac{F'(r)}{r} + x \left[\frac{d}{dr} \frac{F'(r)}{r} \right] \frac{x}{r} = \frac{F'(r)}{r} + \frac{x^2}{r} \frac{rF''(r) - F'(r)}{r^2} , \quad (\text{F.9a})$$

$$\frac{\partial^2 F(r)}{\partial x \partial y} = \frac{\partial}{\partial y} \left[x \frac{F'(r)}{r} \right] = x \left[\frac{d}{dr} \frac{F'(r)}{r} \right] \frac{y}{r} = \frac{xy}{r} \frac{rF''(r) - F'(r)}{r^2} , \quad (\text{F.9b})$$

$$\frac{\partial^2 F(r)}{\partial y^2} = \frac{\partial}{\partial y} \left[y \frac{F'(r)}{r} \right] = \frac{F'(r)}{r} + y \left[\frac{d}{dr} \frac{F'(r)}{r} \right] \frac{y}{r} = \frac{F'(r)}{r} + \frac{y^2}{r} \frac{rF''(r) - F'(r)}{r^2} , \quad (\text{F.9c})$$

Rearranging terms yields

$$\frac{\partial^2 F(r)}{\partial x^2} = \frac{F'(r)}{r} + \frac{x^2}{r^2} \left(F''(r) - \frac{F'(r)}{r} \right) , \quad (\text{F.10a})$$

$$\frac{\partial^2 F(r)}{\partial x \partial y} = \frac{xy}{r^2} \left(F''(r) - \frac{F'(r)}{r} \right) , \quad (\text{F.10b})$$

$$\frac{\partial^2 F(r)}{\partial y^2} = \frac{F'(r)}{r} + \frac{y^2}{r^2} \left(F''(r) - \frac{F'(r)}{r} \right) . \quad (\text{F.10c})$$

Derivatives of the covariances

According to (6.5) the background error covariances read

$$f_{\psi}(r) = (1 - \nu^2) \varepsilon_B^2 L_{\psi}^2 \rho_{\psi\psi}(r) , \quad (\text{F.11a})$$

$$f_{\chi}(r) = \nu^2 \varepsilon_B^2 L_{\chi}^2 \rho_{\chi\chi}(r) , \quad (\text{F.11b})$$

with $\varepsilon_B^2 = V_l = V_t$ and the correlations given by (F.1). The derivatives of the covariances are

$$\rho'_{\psi\psi}(r) = \frac{S'(r) - R'(r)}{2a_{\psi}} = \frac{1}{2a_{\psi}} \left[\frac{J(r)}{r} - rI(r) \right] , \quad (\text{F.12a})$$


$$\rho'_{\chi\chi}(r) = \frac{S'(r) + R'(r)}{2a_{\chi}} = \frac{1}{2a_{\chi}} \left[\frac{J(r)}{r} + rI(r) \right] , \quad (\text{F.12b})$$

and (note that $I'(r)$ is to be evaluated at the lower limit of (F.3) which introduces a minus sign)

$$\begin{aligned} \rho''_{\psi\psi}(r) &= \frac{1}{2a_{\psi}} \left[\frac{rJ'(r) - J(r)}{r^2} - rI'(r) - I(r) \right] = \\ &= \frac{1}{2a_{\psi}} \left[\frac{r^2(\rho_{tt}(r) + \rho_{ll}(r)) - J(r)}{r^2} + r \frac{\rho_{tt}(r) - \rho_{ll}(r)}{r} - I(r) \right] = \\ &= \frac{1}{2a_{\psi}} \left[2\rho_{tt}(r) - \frac{J(r)}{r^2} - I(r) \right] , \end{aligned} \quad (\text{F.13a})$$

$$\begin{aligned} \rho''_{\chi\chi}(r) &= \frac{1}{2a_{\chi}} \left[\frac{rJ'(r) - J(r)}{r^2} + rI'(r) + I(r) \right] = \\ &= \frac{1}{2a_{\chi}} \left[\frac{r^2(\rho_{tt}(r) + \rho_{ll}(r)) - J(r)}{r^2} - r \frac{\rho_{tt}(r) - \rho_{ll}(r)}{r} + I(r) \right] = \\ &= \frac{1}{2a_{\chi}} \left[2\rho_{ll}(r) - \frac{J(r)}{r^2} + I(r) \right] . \end{aligned} \quad (\text{F.13b})$$

Now the corresponding derivatives of the covariances are equal to the derivatives of the correlations (F.12) and (F.13) multiplied by the appropriate factor defined in (F.11).

<div style="display: flex; align-items: center;"> <div style="margin-right: 20px;"> <small>The EUMETSAT Network of Satellite Application Facilities</small> </div> <div>  NWP SAF <small>Numerical Weather Prediction</small> </div> </div>	<h2 style="margin: 0;">Two-dimensional variational ambiguity removal (2DVAR)</h2>	<div style="font-family: monospace; font-size: 0.9em;"> Doc ID : NWPSAF-KN-TR-004 Version : 1.6 Date : 13-08-2021 </div>
--	---	--

Analysis

Substitution of (F.10) to (F.13) in (E.30) yields

$$\begin{aligned}
t(x, y) = & \frac{\varepsilon_B^2}{\varepsilon_0^2 + \varepsilon_B^2} \left[t_0 \frac{v^2 L_X^2}{2a_X} \left\{ -I(r) - \frac{J(r)}{r^2} + 2 \left(\frac{J(r)}{r^2} - \rho_{ll}(r) \right) \frac{x^2}{r^2} \right\} + \right. \\
& + t_0 \frac{(1-v^2)L_\psi^2}{2a_\psi} \left\{ I(r) - \frac{J(r)}{r^2} + 2 \left(\frac{J(r)}{r^2} - \rho_{tt}(r) \right) \frac{y^2}{r^2} \right\} + \\
& \left. + l_0 \frac{v^2 L_X^2}{a_X} \left(\frac{J(r)}{r^2} - \rho_{ll}(r) \right) \frac{xy}{r^2} + l_0 \frac{(1-v^2)L_\psi^2}{a_\psi} \left(-\frac{J(r)}{r^2} + \rho_{tt}(r) \right) \frac{xy}{r^2} \right] , \quad (F.14a)
\end{aligned}$$

$$\begin{aligned}
l(x, y) = & \frac{\varepsilon_B^2}{\varepsilon_0^2 + \varepsilon_B^2} \left[l_0 \frac{(1-v^2)L_\psi^2}{2a_\psi} \left\{ I(r) - \frac{J(r)}{r^2} + 2 \left(\frac{J(r)}{r^2} - \rho_{tt}(r) \right) \frac{x^2}{r^2} \right\} + \right. \\
& + l_0 \frac{v^2 L_X^2}{2a_X} \left\{ -I(r) - \frac{J(r)}{r^2} + 2 \left(\frac{J(r)}{r^2} - \rho_{ll}(r) \right) \frac{y^2}{r^2} \right\} + \\
& \left. + t_0 \frac{(1-v^2)L_\psi^2}{a_\psi} \left(-\frac{J(r)}{r^2} + \rho_{tt}(r) \right) \frac{xy}{r^2} + t_0 \frac{v^2 L_X^2}{a_X} \left(\frac{J(r)}{r^2} - \rho_{ll}(r) \right) \frac{xy}{r^2} \right] . \quad (F.14b)
\end{aligned}$$

From (F.4) to (F.6) it follows that

$$\frac{(1-v^2)L_\psi^2}{a_\psi} = -1 \quad , \quad \frac{v^2 L_X^2}{a_X} = -1 \quad , \quad (F.15)$$

so (F.14) simplifies to

$$\begin{aligned}
t(x, y) = & \frac{\varepsilon_B^2}{\varepsilon_0^2 + \varepsilon_B^2} \left[t_0 \left\{ \frac{J(r)}{r^2} + \left(\rho_{ll}(r) - \frac{J(r)}{r^2} \right) \frac{x^2}{r^2} + \left(\rho_{tt}(r) - \frac{J(r)}{r^2} \right) \frac{y^2}{r^2} \right\} + \right. \\
& \left. + l_0 (\rho_{ll}(r) - \rho_{tt}(r)) \frac{xy}{r^2} \right] , \quad (F.16a)
\end{aligned}$$

$$\begin{aligned}
l(x, y) = & \frac{\varepsilon_B^2}{\varepsilon_0^2 + \varepsilon_B^2} \left[l_0 \left\{ \frac{J(r)}{r^2} + \left(\rho_{tt}(r) - \frac{J(r)}{r^2} \right) \frac{x^2}{r^2} + \left(\rho_{ll}(r) - \frac{J(r)}{r^2} \right) \frac{y^2}{r^2} \right\} + \right. \\
& \left. + t_0 (\rho_{ll}(r) - \rho_{tt}(r)) \frac{xy}{r^2} \right] . \quad (F.16b)
\end{aligned}$$

Double application of 'l Hopital's rule yields

$$\lim_{r \rightarrow 0} \frac{J(r)}{r^2} = \lim_{r \rightarrow 0} \frac{J'(r)}{2r} = \frac{1}{2} J''(0) = 1 \quad , \quad (F.17)$$


since $J''(r) = \rho_{tt}(r) + \rho_{ll}(r) + r(\rho'_{tt}(r) + \rho'_{ll}(r))$ from (F.3). So (F16) is regular at the origin.

Putting $x = r \cos \varphi$ and $y = r \sin \varphi$ makes the terms with $J(r)$ cancel, resulting in

$$t(x, y) = \frac{\varepsilon_B^2}{\varepsilon_0^2 + \varepsilon_B^2} [t_0 (\rho_{ll}(r) \cos^2 \phi + \rho_{tt}(r) \sin^2 \phi) + l_0 (\rho_{ll}(r) - \rho_{tt}(r)) \sin \phi \cos \phi] \quad , \quad (F.18a)$$

$$l(x, y) = \frac{\varepsilon_B^2}{\varepsilon_0^2 + \varepsilon_B^2} [l_0 (\rho_{tt}(r) \cos^2 \phi + \rho_{ll}(r) \sin^2 \phi) + t_0 (\rho_{ll}(r) - \rho_{tt}(r)) \sin \phi \cos \phi] \quad . \quad (F.18b)$$

Along the local x-axis ($\varphi = 0$) or y-axis ($\varphi = \pi/2$) these expressions take a particularly simple form, showing that the shape of the single observation analysis is proportional to the O-B correlations ρ_{ll} and ρ_{tt} , which, of course, should be no surprise.

<p>The EUMETSAT Network of Satellite Application Facilities</p> 	<h1>Two-dimensional variational ambiguity removal (2DVAR)</h1>	<p>Doc ID : NWPSAF-KN-TR-004 Version : 1.6 Date : 13-08-2021</p>
---	--	--

Appendix G Fourier transforms involving a Gaussian function

Forward Fourier transform

Let the function $f(x, y)$ be defined in the spatial domain as a Gaussian function,

$$f(x, y) = F_s e^{-a_s r^2} \quad , \quad (G.1)$$

with $r^2 = x^2 + y^2$ and F_s and a_s constants.

Its Fourier transform in the frequency domain reads (see appendix A)

$$\begin{aligned} \hat{f}(p, q) &= \int_{-\infty}^{\infty} dx \int_{-\infty}^{\infty} dy f(x, y) e^{2\pi i(px+qy)} = \\ &= F_s \int_{-\infty}^{\infty} dx e^{-(a_s x^2 - 2\pi i p x)} \int_{-\infty}^{\infty} dy e^{-(a_s y^2 - 2\pi i q y)} \quad . \end{aligned} \quad (G.2)$$

The integrals over x and y can be evaluated using the relation

$$\int_{-\infty}^{\infty} dz e^{-(Az^2 + Bz)} = \sqrt{\frac{\pi}{A}} e^{-\frac{B^2}{4A}} \quad . \quad (G.3)$$

Some simple algebra yields

$$\hat{f}(p, q) = F_s \frac{\pi}{a_s} e^{-\frac{\pi^2}{a_s}(p^2 + q^2)} \quad . \quad (G.4)$$

Inverse Fourier transform

When deriving an analytical expression for the single observation analysis in Appendix F, the following integrals are needed:

$$I_{pp}(x, y; a) = \int_{-\infty}^{\infty} dp \int_{-\infty}^{\infty} dq p^2 e^{-a(p^2 + q^2)} e^{-2\pi i(px+qy)} \quad , \quad (G.5a)$$

$$I_{pq}(x, y; a) = \int_{-\infty}^{\infty} dp \int_{-\infty}^{\infty} dq pq e^{-a(p^2 + q^2)} e^{-2\pi i(px+qy)} \quad , \quad (G.5b)$$

$$I_{qq}(x, y; a) = \int_{-\infty}^{\infty} dp \int_{-\infty}^{\infty} dq q^2 e^{-a(p^2 + q^2)} e^{-2\pi i(px+qy)} \quad , \quad (G.5c)$$

The integrands are separable in p and q , so

$$I_{pp}(x, y; a) = K_2(x; a) K_0(y; a) \quad , \quad (G.6a)$$

$$I_{pq}(x, y; a) = K_1(x; a) K_1(y; a) \quad , \quad (G.6b)$$



$$I_{qq}(x, y; a) = K_0(x; a) K_2(y; a) \quad , \quad (G.6c)$$

where

$$K_0(x; a) = \int_{-\infty}^{\infty} dp e^{-ap^2 - 2\pi i p x} \quad , \quad (G.7a)$$

$$K_1(x; a) = \int_{-\infty}^{\infty} dp p e^{-ap^2 - 2\pi i p x} \quad , \quad (G.7b)$$

$$K_2(x; a) = \int_{-\infty}^{\infty} dp p^2 e^{-ap^2 - 2\pi i p x} \quad . \quad (G.7c)$$

 	Two-dimensional variational ambiguity removal (2DVAR)	Doc ID : NWPSAF-KN-TR-004 Version : 1.6 Date : 13-08-2021
---	--	---

The integral K_0

Write (G.7a) as

$$K_0(x; a) = \int_{-\infty}^{\infty} dp \ e^{-ap^2} (\cos(2\pi xp) - i \sin(2\pi xp)) \quad . \quad (G.8)$$

The second term yields zero, since the sine is odd while the Gaussian is even. The first term can be evaluated using equation (7.4.6) of *Abramowitz and Stegun* [1970] and yields

$$K_0(x; a) = \sqrt{\frac{\pi}{a}} e^{-\frac{\pi^2 x^2}{a}} \quad . \quad (G.9)$$

The integral K_1

There are several ways that integral K_1 can be evaluated. One way is to split the complex exponential into a sine and a cosine, like in (G.8) and do partial integration. A simpler way is to observe that from (G.7a)

$$\frac{dK_0(x; a)}{dx} = \frac{d}{dx} \int_{-\infty}^{\infty} dp \ e^{-ap^2 - 2\pi i p x} = -2\pi i \int_{-\infty}^{\infty} dp \ p e^{-ap^2 - 2\pi i p x} = -2\pi i K_1(x; a) \quad , \quad (G.10)$$

so that

$$K_1(x; a) = \frac{-1}{2\pi i} \frac{dK_0(x; a)}{dx} \quad . \quad (G.11)$$

Substitution of (G.9) in the right hand side of (G.11) gives

$$K_1(x; a) = -i \left(\frac{\pi}{a}\right)^{3/2} x e^{-\frac{\pi^2 x^2}{a}} \quad . \quad (G.12)$$

The integral K_2

Double differentiation of (G.7a) yields

$$\frac{d^2 K_0(x; a)}{dx^2} = \frac{d^2}{dx^2} \int_{-\infty}^{\infty} dp \ e^{-ap^2 - 2\pi i p x} = (-2\pi i)^2 \int_{-\infty}^{\infty} dp \ p^2 e^{-ap^2 - 2\pi i p x} = -4\pi^2 K_2(x; a) \quad , \quad (G.13)$$

so that

$$K_2(x; a) = \frac{-1}{4\pi^2} \frac{d^2 K_0(x; a)}{dx^2} \quad . \quad (G.14)$$

With (G.9) this yields


$$K_2(x; a) = e^{-\frac{\pi^2 x^2}{a}} \left[-\left(\frac{\pi}{a}\right)^{5/2} x^2 + \frac{1}{2} \left(\frac{\pi}{a^3}\right)^{1/2} \right] \quad . \quad (G.15)$$

The integrals I_{pp} , I_{pq} , and I_{qq}


Substitution of (G.9), (G.12) and (G.15) in (G.6) yields

$$I_{pp}(x, y; a) = \left[-\left(\frac{\pi}{a}\right)^3 x^2 + \frac{1}{2} \frac{\pi}{a^2} \right] e^{-\frac{\pi^2(x^2+y^2)}{a}} \quad , \quad (G.16a)$$

$$I_{pq}(x, y; a) = -\left(\frac{\pi}{a}\right)^3 x y e^{-\frac{\pi^2(x^2+y^2)}{a}} \quad , \quad (G.16b)$$

<div data-bbox="140 129 255 185"> The EUMETSAT Network of Satellite Application Facilities </div> <div data-bbox="284 138 550 212">  NWP SAF Numerical Weather Prediction </div>	<h1>Two-dimensional variational ambiguity removal (2DVAR)</h1>	Doc ID : NWPSAF-KN-TR-004 Version : 1.6 Date : 13-08-2021
--	--	---

$$I_{qq}(x, y; a) = \left[-\left(\frac{\pi}{a}\right)^3 y^2 + \frac{1}{2} \frac{\pi}{a^2} \right] e^{-\frac{\pi^2(x^2+y^2)}{a}} . \quad (\text{G.16c})$$

<p>The EUMETSAT Network of Satellite Application Facilities</p> 	<h1>Two-dimensional variational ambiguity removal (2DVAR)</h1>	<p>Doc ID : NWPSAF-KN-TR-004 Version : 1.6 Date : 13-08-2021</p>
---	--	--

Appendix H Minimization step size

The minimization is performed by routine LBFGS [Liu and Nocedal, 1989]. The algorithm adapts its step size, but the size of the first step must be given. The minimization starts at the point $\xi = 0$. At this point the cost function value $f(0)$ and its gradient $g(0)$ are known.

Suppose now that the cost function is a parabola in the plane defined by the gradient direction and the minimum. The cost function then reads

$$f(\xi) = a\xi^2 + b\xi + c \quad , \quad (H.1)$$

with gradient

$$g(\xi) = \frac{df(\xi)}{d\xi} = 2a\xi + b \quad . \quad (H.2)$$

The minimum is located at $\xi = \xi_{min}$ where the gradient equals zero. Equation (H.2) immediately yields

$$\xi_{min} = -\frac{b}{2a} \quad (H.3)$$

Substitution of (H.3) in (H.1) gives the value of the cost function at the minimum

$$f(\xi_{min}) = c - \frac{b^2}{4a} \quad (H.4)$$

The value of ξ_{min} from (H.3) is expected to give a good first guess for the initial step size. Since the minimization starts at $\xi = 0$, (H.1) and (H.2) readily yield

$$c = f(0) \quad , \quad b = g(0) \quad . \quad (H.5)$$

One extra relation is needed to fix the coefficients of the parabola. This needs some additional assumption. The Single Observation Analysis shows that

$$f(\xi_{min}) = \frac{1}{2}f(0) \quad (H.6)$$

In practical cases, the minimum value of the cost function turns out to be 25% to 90% of its initial value.


Substitution of (H.4) and (H.5) into (H.6) gives

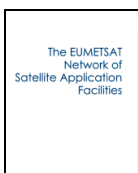

$$a = \frac{g^2(0)}{2f(0)} \quad . \quad (H.7)$$

Substitution of (H.7) into Equation (H.3) gives the final result

$$\Delta\xi = |\xi_{min}| = \frac{f(0)}{|g(0)|} \quad (H.8)$$


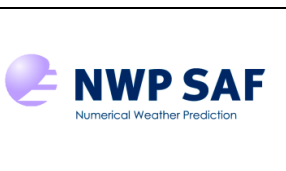
for the initial step size. 2DVAR obtains the best results when the step size in (H.8) is multiplied by a factor of 30.

<p>The EUMETSAT Network of Satellite Application Facilities</p> 	<h1>Two-dimensional variational ambiguity removal (2DVAR)</h1>	<p>Doc ID : NWPSAF-KN-TR-004 Version : 1.6 Date : 13-08-2021</p>
---	--	--

 	Two-dimensional variational ambiguity removal (2DVAR)	Doc ID : NWPSAF-KN-TR-004 Version : 1.6 Date : 13-08-2021
--	--	---

References

- Abramowitz, M. and I.A. Stegun, 1970.
Handbook of mathematical functions.
Dover Publications, new York, U.S.A.
- Bonavita, M., L. Isaksen, and E. Hólm, 2012.
On the use of EDA background error variances in the ECMWF 4D-Var.
Q. J. R. Meteor. Soc. 137, 1540-1559.
- Daley, R., 1991,
Atmospheric Data Analysis.
Cambridge University Press, Cambridge, New York, USA.
- Errico, R.M., 1997,
What is an adjoint model?
Bulletin of the American Meteorological Society, 2577-2591.
- Giering, R., and Kaminski, T., 1998,
Recipes for adjoint code construction.
ACM Transactions on Mathematical Software, 24, 437-474.
- Lin, W., M. Portabella, A. Stoffelen, J. Vogelzang, and A. Verhoef, 2016,
On mesoscale analysis and ASCAT ambiguity removal.
Q. J. Royal Meteorol. Soc. 142, 1745-1756. doi: 10.1002/qj.2770.
- Liu, D.C., and Nocedal, J., 1989,
On the limited memory BFGS method for large scale optimization methods.
Mathematical Programming, 45, pp. 503-528.
- Lorenc, A.C., 1986,
Analysis methods for numerical weather prediction.
Q. J. Royal Meteorol. Soc., 112, 1177-1194
- Portabella, M., 2002,
Wind retrieval from satellite radar systems.
Thesis, University of Barcelona, Barcelona, Spain.
- Press, W.H., Flannery, B.P., Teukolsky, S.A., and Vetterling, W.T., 1988,
Numerical recipes in C.
Cambridge University Press, Cambridge, New York, USA.
- Stoffelen, A.C.M., and Anderson, D.L.T., 1997,
Ambiguity removal and assimilation of scatterometer data.
Q. J. Roy. Meteorol. Soc. 123, pp. 491 – 518.
- Stoffelen, A.C.M., 1998,
Scatterometry.
Thesis. Universiteit Utrecht, Utrecht, The Netherlands.

 	<h1>Two-dimensional variational ambiguity removal (2DVAR)</h1>	<p>Doc ID : NWPSAF-KN-TR-004 Version : 1.6 Date : 13-08-2021</p>
---	--	--

Verhoef, A., J. Vogelzang, J. Verspeek, and A. Stoffelen, 2018a,
AWDP top level design, version 3.2.
Report NWPSAF-KN-DS-004, UKMO, UK.

Verhoef, A., J. Vogelzang, J. Verspeek, and A. Stoffelen, 2018b,
PenWP top level design, version 2.2.
Report NWPSAF-KN-DS-001, UKMO, UK.

Vogelzang, J., 2006,
The orientation of SeaWinds wind vector cells.
Report NWPSAF-KN-TR-003, UKMO, UK.

Vogelzang, J. and A. Stoffelen, 2011,
NWP model error structure functions obtained from scatterometer winds.
IEEE Trans. Geosci. Rem. Sens., doi: 10.1109/TGRS.2011.2168407.

Vogelzang, J., 2019,
An improved 2DVAR batch grid.
Report SAF/OSI/CDOP3/KNMI/TEC/TN/339, EUMETSAT.

De Vries, J., Stoffelen, A., and Beysens, J.,
Ambiguity removal and product monitoring for SeaWinds.
Report NWPSAF-KN-TR-001, UKMO, UK.